NASA-TM-76931

NASA TECHNICAL MEMORANDUM

NASA TM-76931

A SURVEY OF THE THREE-DIMENSIONAL HIGH REYNOLDS NUMBER TRANSONIC WIND TUNNEL

Kazuaki Takashima, Hideo Sawada, Takeo Aoki

Translation of "Koku Uchi Gijutsu Kenkyujo Shiryo," National Aerospace Laboratory, Tokyo, Japan. NAL-TM-440 August 1981, pp. 1-38

NATIONAL AERONAUTICS AND SPACE ADMINISTRATION
WASHINGTON, DC 20546 JUNE 1982

STANDARD TITLE PAGE

1. Report No. NASA TM-76931	2. Government Accession No.	3. Recipient's Catalog No.
4. Title and Subtitle: A SURVEY OF THE THREE-DIMENSIONAL HIGH REYNOLDS NUMBER TRANSONIC WIND TUNNEL		5. Report Date: June 1982 6. Performing Organization Code
7. Author(s): Kazuaki Takashima, Hideo Sawada, Takeo Aoki National Aerospace Laboratory		8. Performing Organization Report No. 10. Work Unit No.
9. Performing Organization Name and Address: Leo Kanner Associates, Redwood City, California 94063		11. Contract or Grant No. NASw- 3541 13. Type of Report and Period Covered: Translation
12. Sponsoring Agency Name and Address: National Aeronautics and Space Administration Washington, D.C. 20546		14. Sponsoring Agency Code

15. Supplementary Notes

Translation of "Koku Uchi Gijutsu Kenkyujo Shiryo," National Aerospace Laboratory, Tokyo, Japan. NAL-TM-440 August 1981, pp. 1-38

16. Abstract

A survey of the facilities for aerodynamic testing of airplane models at transonic speeds and high Reynolds numbers is presented. At first, the need for high Reynolds number testing is reviewed, using some experimental results. Then, some new approaches to high Reynolds number testing, i.e., the cryogenic wind tunnel, the induction driven wind tunnel, the Ludwieg tube, the Evans clean tunnel and the hydraulic driven wind tunnel are described. Finally, this paper comments upon the level of development of high Reynolds number testing facilities in this country.

17. Key Words (Selected by Author(s))	18. Distribution Statement: "Unclassified-Unlimited"		
19. Security Classif. (of this report)	20. Security Classif. (of this page)	21. No. of Pages	22.

NASA HQ

TABLE OF CONTENTS

A Survey of the Three-Dimensional High Reynolds Number Transonic Wind Tunnel

K. Takashima, H. Sawada, T. Aoki

National Aerospace Laboratory

1. Introduction

This report constitutes a summary of the results of surveys on transonic wind tunnel facilities for high Reynolds number tests. The aircraft industry is a so-called high technology industry, and the fact that it is a very important technical field for Japan which aims to be a technically advanced country is obvious. Clarification of the aerodynamic properties and precise predicting of the aerodynamic performance of an aircraft are the most important aspects in the development of aircraft. However, evaluation of the aerodynamic force acting on an aircraft is not so easy, although this depends on each case. In particular, when the flow field in the vicinity of an aircraft travelling near the speed of sound is a transonic flow field, a formula which expresses the flow field would exhibit extreme non-linearity, and many researchers have devoted considerable effort to its solution.

One method of studying the aerodynamic properties of an aircraft would be a theoretical method in which an analytical model of the flow field is formulated using such a non-linear formular followed by determination of various properties through solution of the formula. Another method would be that in which the flow field is simulated, and in which the properties of difficulty are experimentally determined. Wind tunnel testing (1, 2) is the most widely used experimental method of problem solving

"Numbers in the margin indicate pagination in the foreign text"

In recent years, estimation of the aerodynamics of an aircraft during transonic flight has become possible by numerical solution through the marked development of computers, but the flow models treat idealized potential flows or treat aircraft configurations in extremely simplified forms. Thus, replacement of wind tunnel tests with the Navier·Stokes equation which expresses the actual flow on actual configurations would be impossible in the near future [3,4]. Rather, such numerical methods complement wind tunnel tests and provide guidelines for solution of problems when wind tunnel tests are difficult. Consequently, wind tunnel tests must be relied on to predict the aerodynamics during high speed flight.

Thus, the significance of wind tunnel tests from the era of the Wright brothers to the present has not been lost. To the /2
contrary, its importance has increased. These days, wind tunnel tests lasting thousands of hours are carried out for the development of a new aircraft, and reliance on wind tunnel test data has increased. Thus, can the precise flight state be reproduced in wind tunnel tests to the degree anticipated, and can the aerodynamic properties of the aircraft be predicted? While this varies with the case, the answer is not always yes.

The development of the method of similar flow fields using wind tunnels clearly lags behind the marked development to date of aircraft. The Mach number, which is a parameter illustrating the effects of compressibility of air, has attracted considerable interest when the phenomenon of high speed flow accompanying increased aircraft speed must be studied. Of course, changes in the flow field due to changes in the Mach number are marked, and similarity in the flow field cannot be considered while underrating the Mach number. As a result, while the similarity of compressibility effects has been established at equal Mach numbers, the similarity of the other parameters, for instance,

Reynolds number, which illustrates the viscosity or dimensional effect, has been disregarded. That is because it has been very difficult to produce similar Mach numbers and Reynolds numbers in flight tests in wind tunnels, and because the similarity of the Reynolds number in high speed air flow is less important than that of the Mach number.

The blame for underrating the similitude of the Reynolds number is realized in the discovery of great differences between the wind tunnel test results and flight test results in the construction of the C-141 transport by the U.S. Air Force. Considerable expense and time were spent in modification of the aircraft.

Many wind tunnel test Reynolds numbers at present are one order of magnitude lower than the numbers during actual flight, and wind tunnel tests are impossible on large aircraft with similar Reynolds number and Mach number. The necessity [5,6] of tests in which these two parameters are similar is explained in detail below, and this has been recognized in Europe and America, especially in transonic regions. The means of implementation have been evaluated in the United States and in AGARD countries [7,8,9], and a wind tunnel (NTF, National Transonic Facility) has already been constructed for this purpose in the United States.

First, we will explain the necessity of transonic, high Reynolds number tests while citing actual examples, followed by evaluation while introducing problems accompanying high Reynolds number tests and concrete proposals for their solution. Finally, we will consider facilities in Japan which are suitable for high Reynolds number transonic tests.

2. Necessity of High Reynolds Number Transonic Tests

2.1 On the Principle of Similarity

As is well known, since one flow of viscous fluid is kinetically similar to another flow, the Reynolds numbers must be identical. This signifies that the ratio between the force of inertia and the viscous force of both fluids is identical. Specifically,

$$\left(\frac{\text{force of inertia}}{\text{viscous force}}\right)_{I} = \left(\frac{\text{force of inertia}}{\text{viscous force}}\right)_{II}$$

This means that the following formula

$$\frac{m\dot{V}}{\mu(du/dy)} \sim \frac{\rho V^2 l^2}{\mu V l} \sim \frac{\rho V l}{\mu} \quad \text{Reynolds Number}$$

is a constant.

Furthermore, the ratio of forces due to the force of inertia and pressure must also be equal for two fluids to maintain similarity. These conditions would be automatically satisfied if the Reynolds number were equal in steady fluids.

Next, similitude of the Reynolds number alone is insufficient in high speed air flow such as transonic flows, and the principle of similitude of compressible fluids must also be considered while considering the elastic force due to the compressibility of air. In short, the ratio between the force of inertia and the elastic force must be equal in two flows. Specifically,

$$\left(\frac{\text{force of inertia}}{\text{elastic force}}\right)_{I} = \left(\frac{\text{force of inertia}}{\text{elastic force}}\right)_{II}$$

This means that the following formula

$$\frac{m\dot{V}}{El^2} \sim \frac{\rho V^2 l^2}{El^2} \sim \frac{\rho V^2}{E} \sim \frac{V^2}{a^2} = M^2 \quad \text{Square of Mach Number}$$

develops, and the Mach number must be maintained at a constant.

As a result, identical values must be selected for the two parameters of the Reynolds number and the Mach number in the flight state for the flow of a transonic wind tunnel to resemble the true flight state.

2.2 Sensitivity to Reynolds Number

Since the Reynolds number is a parameter of similitude related to the viscosity, the phenomenon when a viscous flow along the surface of a body plays an important role in determination of the force and moment is sensitive to changes in the Reynolds number. There are many such cases, as illustrated in table 2.1 [9]. The items illustrated in the table are divided into two general cases. One is the case of dimensional effect and the other is the case in which there is a strong correlation between the viscous flow on the surface of a body and the external potential flow. Heat transfer (no problem in the transonic region) and surface friction belong to the former, while the latter is a flow in which separation occurs. /3

TABLE 2.1 PHENOMENON OF SENSITIVITY TO REYNOLDS NUMBER IN VARIOUS AIRCRAFT [9]

	1 現象 ＼ 2 飛行体	3 各種飛行物体				
		4 曲技飛行体	5 亜音速輸送機	6 超音速機	7 極超音速機	8 打上げロケット等
9	境界層発達，剝離	○	○	○	○	○
10	境界層遷移		○	○	○	
11	乱流境界層	○	○	○	○	○
12	境界層～衝撃波干渉	○	○	○	○	○
13	剝離流	○			○	○
14	粘性剪断流	○	○	○	○	○
15	粘性コーナー流	○				
16	粘性混合効果	○	○	○	○	○
17	底面流とウエーク	○	○	○	○	○
18	底面再循環流				○	○
19	底面抵抗				○	○
20	表面摩擦	○	○	○		
21	粗さ，突起物の抵抗	○	○	○	○	○
22	圧力変動	○				○
23	渦流	○	○	○	○	○
24	干渉流領域	○	○	○	○	○
25	ジェットプルーム	○	○	○	○	○
26	ブラフボディ				○	○
27	熱伝達				○	○

1 phenomenon
2 vehicles
3 various types of vehicles
4 aerobatic aircraft
5 subsonic transport
6 supersonic aircraft
7 hyper-sonic aircraft
8 launched rocket
9 development of boundary layer, separation
10 transition of boundary layer
11 turbulent boundary layer
12 boundary layer-shock wave interaction
13 separating flow
14 viscous shear flow
15 viscous corner flow
16 viscous mixing effect
17 base flow and wake
18 base recirculating flow
19 base drag
20 surface friction
21 coarseness, drag of protuberance
22 pressure fluctuation
23 eddy flow
24 interference flow region
25 jet plume
26 bluff body
27 heat transfer

Surface friction can be extrapolated to a certain degree if the flow is turbulent and if separation does not occur. While commonly used, roughness can be applied, thereby hastening the boundary layer transition and resulting in comparatively reliable drag data. However, in low Reynolds number tests, the turbulent boundary layer on the flow side above the wing surface is relatively thick, and there is interference with the shock wave. Thus, estimations of the pitching moment coefficient would be imprecise (refer to section 2.4.2).

Next, while separation and the accompanying drag increases etc. are very sensitive to the Reynolds number, the state at a high Reynolds number cannot be extrapolated at present as in the case of the previous drag. Figure 2.1 illustrates a typical case of the transonic flow around a wing, but the problem of separation at a certain degree of the shock wave develops.

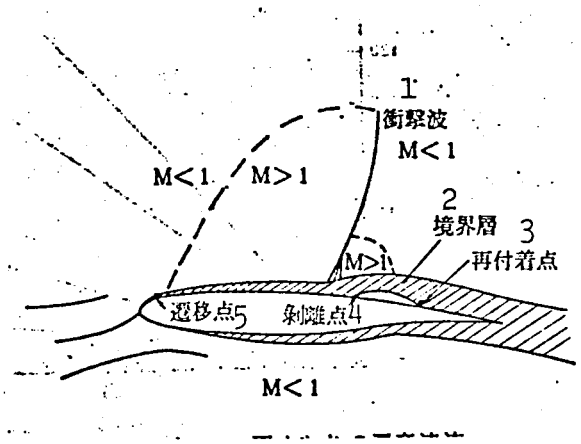

Figure 2.1 Transonic flow around wing

1 shock wave
2 boundary layer
3 point of reattachment
4 separation point
5 transition point

2.3 Present State of Reynolds number Similarity in Wind Tunnel

/4

Figure 2.2 [9] illustrates the state of similarity in the United States according to wind tunnels. While the material is fairly old, the state of the wind tunnel is virtually unchanged. These aircraft planned in 1969 include the current jumbo jet as well as large cargo planes and large supersonic aircraft. As

indicated in figure 2.2, the Reynolds number of tests in existing wind tunnels is less than 1/10 the Reynolds number of transonic flight, and the similarity is poor for the aforementioned reasons.

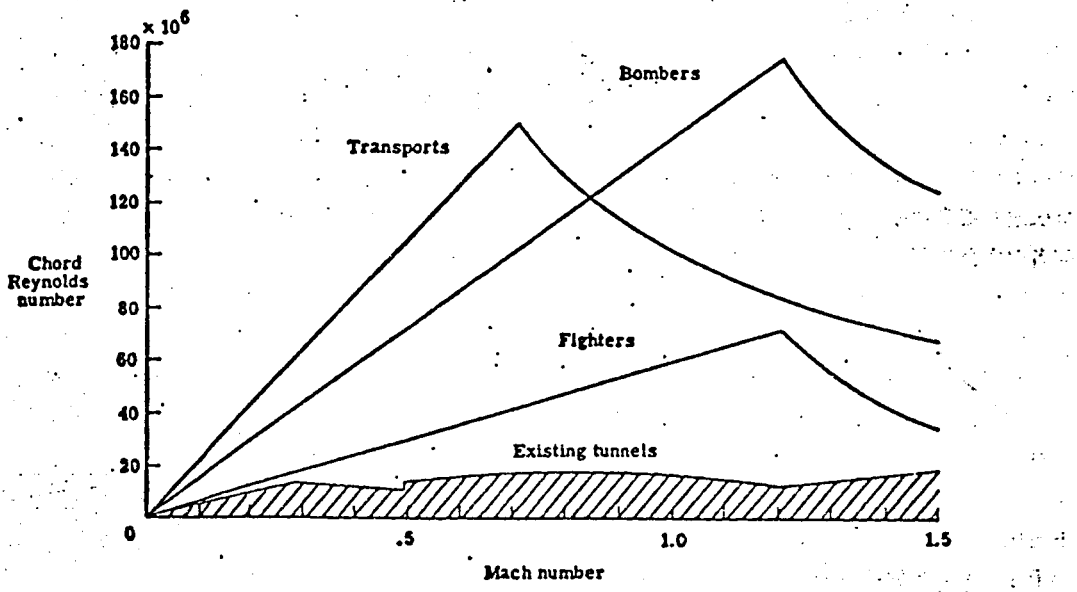

Figure 2.2 State of similarity of Reynolds number in wind tunnels [9]

The conditions in Europe are the same as those in figure 2.2. Evaluations of these problems have been carried out for some time in the AGARD countries [10].

There are very few wind tunnels in Japan which are capable of transonic testing of full-scale models. The only ones available are the 2 m x 2 m wind tunnel at the National Aerospace Laboratory (capable of Reynolds number of 2×10^6) and the 0.6 m x 0.6 m wind tunnel (Reynolds number of 1.5×10^6) at Mitsubishi Heavy Industries. This problem will be discussed in chapter 5.

2.4 Examples of Problems Arising from Differences in Reynolds Number

As previously indicated, the wind tunnel test Reynolds number is one order of magnitude smaller than the flight Reynolds number in the transonic region. Because of this, there are cases in which the performance forecast in wind tunnel tests differs greatly from actual performance in aircraft development, and numerous problems have already developed. These are illustrated in table 2.2 [9]. Typical examples in which the Reynolds number effect has an influence on the individual aerodynamic properties are explained below.

Table 2.2 Problems due to Reynolds number effect which have been discovered in flight tests [9]

Aircraft	Problems
C-141	Errors in forecasting the flow on the wing surface. These affected the stability, load and properties. Structural reevaluation tests and modifications took one year and millions of dollars.
F-111	Failure to forecast the interference effect of the transonic flow. Under-evaluation of resistance. Vast sums were used for redesign and modification.
B-58	Unsuitable aerodynamic optimization of transonic velocity.
B-70	The acceleration margin at low transonic rates affected the
YF-12	flight range and handling, thereby reducing the effectiveness of the aircraft.
F-102	Error in emanation of transonic resistance, resulting in replacement by F-106. Both aircraft are plagued by base resistance at transonic speeds.
Civilian aircraft	Redesign was required in two types of jet transports due to interference of the flow between the engines and the wind surfaces. In many cases, the pitching moment, drag and maximum lift presumptions were ambiguous.

2.4.1 Pressure Distribution on Wing Surface [11] /5

Figure 2.3 illustrates the results acquired from the C-141 transport which are well known. As illustrated in figure (b), the pressure distribution from wind tunnel test results differs greatly from the flight test results. In low Reynolds number tests (wind tunnel tests), the relatively turbulent boundary layer is thick (proportional to (1/5) the Reynolds number), as

illustrated in figure 2.4, and the position of the shock wave advances approximately 20% in comparison to high Reynolds number tests due to interference from external local supersonic regions. This alters the pressure distribution, including a change of 11% in the pitching moment. The result of this erroneous performance forecast was a nine month delay in use of the aircraft, reanalysis of the structure and loading of ballast weight etc.

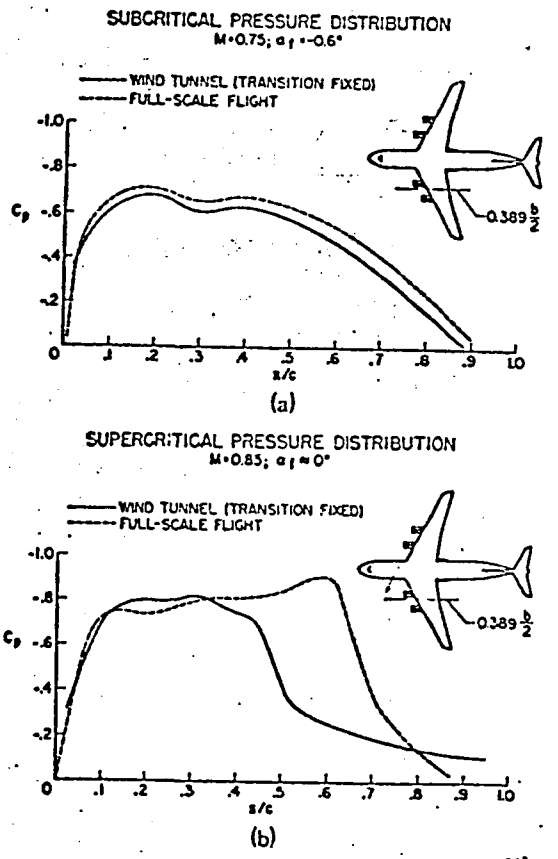

Figure 2.3 Differences in pressure distribution based on Reynolds number [11]

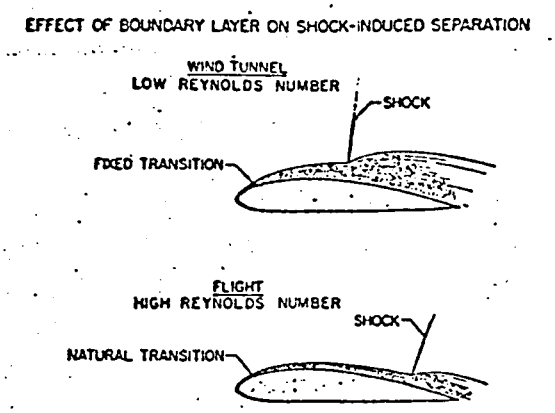

Figure 2.4 Effects of differences in the boundary layer in wind tunnel tests and flight tests [11]

As seen in figure 2.3 (a), there is also a case (subcritical) in which there is no effect due to differences in the Reynolds number. Thus, the phenomenon seen in figure 2.3 (b) is not usually seen.

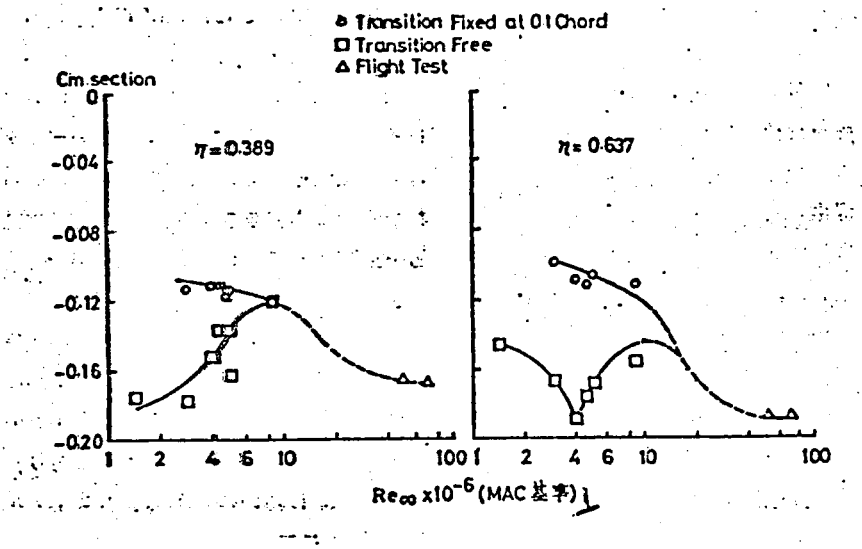

Figure 2.5 Changes in pitching moment coefficient due to Reynolds number M = 0.825, C_L = 0.4 [12]

1. MAC standards

2.4.2 Pitching Moment Coefficient

/6

Figure 2.5 [12] illustrates an example of change in the pitching moment coefficient C_m based on the Reynolds number. As this figure indicates, the value of C_m obtained by the technique of fixed transition (use of roughness) which is used extensively in wind tunnel tests at low Reynolds number is a value which differs considerably from the value of C_m obtained in flight tests. However, convergence to the flight test values could be anticipated if the wind tunnel test Reynolds number could be increased.

The wind tunnel test values based on the free transition method approach the values of C_m of flight tests more than the values of C_m obtained by the fixed transition method, but this is

because the boundary layer is relatively thin due to free transition, resulting in a more posterior location of the shock wave than in the case of fixed transition. Since the position of the boundary layer transition shifts to the upstream side when the Reynolds number increases, the results become identical with those from fixed transition. It is impossible to determine whether the free transition or fixed transition test method is the more precise simulation method when there is separation inducing a shock wave if there are no flight test results, in short, if there are no results from high Reynolds number tests.

2.4.3 Position of Shock Wave

As previously stated, the position of the shock wave on the wing surface varies due to differences in the Reynolds number or differences in the test method. Figure 2.6 [13] illustrates this. This figure illustrates the shift of the position of the shock wave on the upper surface of two types of wings when the boundary layer near the leading edge undergoes forced transition, the angle of attack as well as the Mach number are held constant and the Reynolds number is altered. The position of the shock wave varies by 5 to 19% of the wing chord length when the Reynolds number is altered from 2×10^6 to 8×10^7. Such a change in the position of the shock wave is a phenomenon seen only in Reynolds number ranges of 10^6 to 10^8, and the virtual absence of change in the position of the shock wave at other Reynolds number ranges can be forecast from figure 2.6.

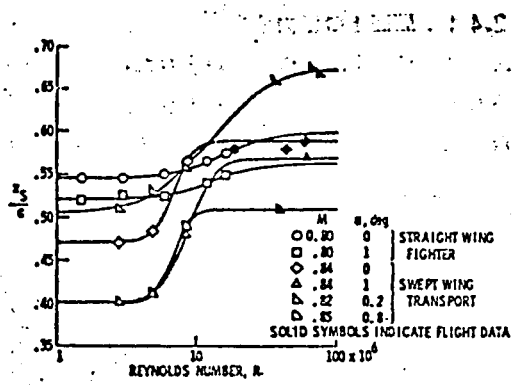

Figure 2.6 Change in position of shock wave due to Reynolds number [13]

2.4.4 Drag Coefficient

Figure 2.7 [14] illustrates changes in the drag coefficient of full-scale models based on the Reynolds number. In this figure, the values of the drag coefficient C_D from the wind tunnel test results differ considerably from the flight results. The difference is very important in operations of aircraft, and can lead to serious errors in calculated fuel consumption and weight of the payload. Consequently, forecast of the C_D to high precision (± 0.0002) based on wind tunnel tests is required for aircraft design and production [12]. In addition, the extrapolated values of the wind tunnel test results from figure 2.7 virtually match the flight test results at Reynolds number of (40 to 50) x 10^6. A Reynolds numbers of 40 x 10^6 (60 x 10^6 flight Reynolds number of Boeing 727) is used as the standard in high Reynolds number tests since the change in C_D is slight at higher Reynolds numbers, and that value is used in the specifications [15] of the large AGARD wind tunnel.

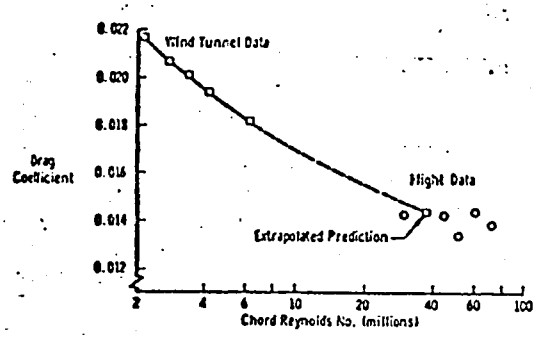

Figure 2.7 Effect of Reynolds number on drag coefficient

Figure 2.8 [9] illustrates the effects of the Reynolds number on the drag coefficient of the fuselage to the rear of the engine. The data are from a full-scale model in which interference from the walls of the wind tunnel cannot be ignored, but even if that is excluded, presumption of the values of the flight test data from the wind tunnel test results would be difficult.

2.4.5 Lift Coefficient

The effects of the Reynolds number on the lift coefficient are important not only in the case of cruising anticipated from figure 2.3 (b) but also in the case of high lift, although this is in low speed regions. At low Reynolds numbers, the boundary layer is a laminar flow, and differences arise because separation is difficult at high Reynolds numbers due to the formation of a turbulent boundary layer while separation readily occurs in regions of inverse pressure slope. /7

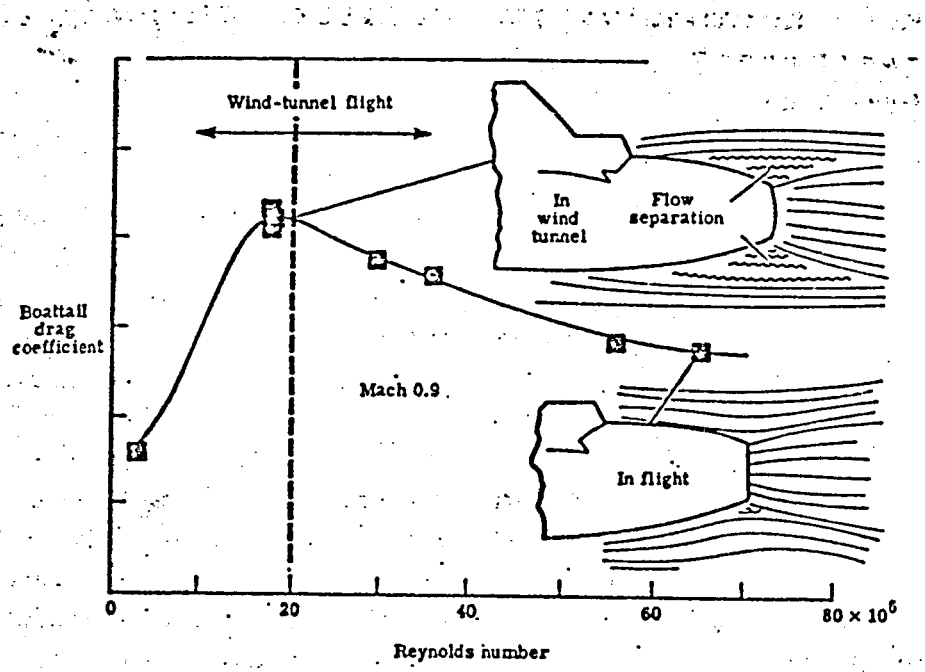

Figure 2.8 Drag of fuselage behind the engine and Reynolds number [9]

Figure 2.9 [12] illustrates the effects of the Reynolds number on the incremental lift coefficient. The data from wind tunnel tests resemble the flight test data, excluding the middle stage figure of figure 2.9 (b), but that is not the case for the middle stage figure (b). When the difference of the magnitude of the figure is the incremental lift coefficient, it corresponds to 10% of the coefficient of lift during landing. An aircraft with a wing larger than necessary would be designed and produced. A 10% reduction in the wing area of aircraft of the DC-10, L-1011 class would signify a fuel reduction of 1.8 tons in a flight between San Francisco and New York, and the payload could be increased. In addition, the amount of reduction in one flight by one aircraft, even if slight, would greatly reduce the amount of fuel and the expense world-wide considering the total flight distance for the mean number of years of service of the aircraft and the total amount of aircraft produced.

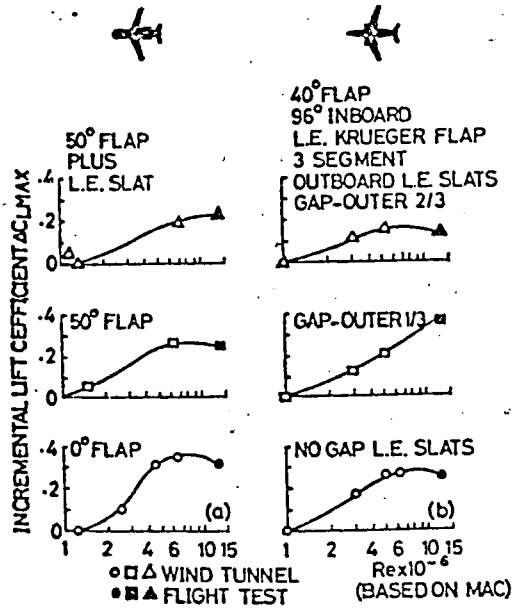

Figure 2.9 Effect of Reynolds number on incremental lift coefficient [12]

There are many cases in which the wind tunnel test data cannot accurately forecast the flight test performance due to the disagreement of Reynolds numbers as stated in this section. There are thus cases in which the attendant problems simply must be solved as well as cases in which unnecessarily extravagant specifications result due to under-evaluation of performance. In the former case, the necessity of considerable expense and time for the solutions is clarified in table 2.2. In the case of extravagant specifications, operations are usually continued with waste so long as there are no repairs.

However, the Reynolds number of wind tunnel tests cannot be increased easily to the same degree as the flight Reynolds number, and there are problems such as the construction cost and costs to maintain operations because the facilities are of large scale, in addition to technical problems such as the load of a /8 wind tunnel model (70 kg/mm^2) [7] and the energy for driving the

wind tunnel (electric motor of 10,000-odd kilowatts). The next chapter briefly explains the technical difficulties.

3. Problems in Acquisition of High Reynolds Numbers

The fact that a flow field corresponding to a very large Reynolds number ($R_c \geq 5 \times 10^7$)[16] must be produced in the wind tunnel test section to precisely determine the aerodynamic performance of aircraft to be developed in wind tunnel tests was indicated in the previous section. However, there is still no operating wind tunnel which produces such flow fields (one is under construction in the United States [17], and one is planned in Europe [18].). In one concept, if a model installed in a wind tunnel were made to full-scale dimensions, and if a uniform flow of the wind tunnel were produced at the flight velocity of an actual aircraft, very reliable wind tunnel tests would be possible if a wind tunnel capable of enclosing a full-scale model were constructed since the Reynolds number of the flow field in the test section would coincide with that of an actual aircraft (the distortion of test data due to interference from the wind tunnel walls etc. should be contained within the experimental accuracy.). At low speeds, construction of a wind tunnel capable of handling a full-scale model would be in the range of the possible, but at cruising transonic regions of actual transport, production of such a large scale transonic wind tunnel would be impossible because of the drive energy required. Furthermore, the production expense and time of the full-scale model would have to be added, and the technical equipment for the construction would also have to be large scale. This would be inconvenient and uneconomical in aircraft development. Research has been conducted on wind tunnels capable of producing a flow field with a high Reynolds number at a convenient size using small power based on such a concept. The ejection type of wind tunnel has long been used as the wind tunnel capable of satisfying such requirements simply, but this type of wind tunnel is inferior to the continuous circulation type wind tunnel in

terms of the capacity to produce data necessary for development, and a wind tunnel for development must be approached [16]. Thus, this chapter discusses only the continuous type wind tunnel.

There are three methods, given below, of obtaining a flow field with a high Reynolds number at low power [2].

1° raising the stagnation pressure.
2° using material with great molecular weight as the internal fluid.
3° reducing the stagnation temperature.

When the ratio between the size of the model (typical wing chord length $\bar{c}$) and the size of the cross sectional area of the test section ($\sqrt{A_W}$, A_W: cross sectional area of test section) is held constant (the magnitude of interference by the wind tunnel walls corresponds to a virtual constant.), the power required to produce a flow with a mach number and Reynolds number set in a given measurement section would be generally expressed as

$$\text{Power} \propto \frac{\mu_0^2 a_0^3}{\gamma P_0} \qquad (1)$$

Here, γ, μ, a and P represent the specific heat ratio of fluid in the wind tunnel, the viscosity coefficient, speed of sound and pressure respectively. The subscript 0 represents the various quantities at the stagnation point. Only air is considered as the flow in the wind tunnel since the discussion in this paper centers on transonic wind tunnels. Furthermore, γ is virtually constant when the gas used in the wind tunnel is determined, and μ_0, a_0 become functions only of temperature. Thus, when the temperature is held constant and only the stagnation pressure P_0 is altered, the following relation is derived from equation (1).

$$\text{Power} \propto \frac{1}{P_0} \qquad (2)$$

Specifically, when the stagnation pressure is increased, the flow field of a prescribed Mach number and Reynolds number can be implemented in the test section with less power. The dimensions of the model must be reduced in inverse proportion to the stagnation pressure in order to maintain the same Reynolds number even when the stagnation pressure is raised. This reduction in the model dimensions necessitates reduction in the dimensions of the model struts. However, the stress within the model struts and the model produced by the force of air to which the model is subjected increases proportionally to the stagnation pressure. For this reason, the model struts must be increased proportionally to the model. Furthermore, the strength of the model must be raised so that the amount of distortion of the model itself does not increase. As a result, there would naturally be an upper limit to the stagnation pressure. Furthermore, when the stagnation pressure is raised, the problem of requiring the wind path itself to be pressure resistant would remain even if the force required to drive the wind tunnel were reduced. Dynamic pressure below 200 kPa would be desirable in wind tunnel tests of transport shapes [17]. There is a limit to the rise of the stagnation pressure (Figure 3.1).

Conversely, the following equation results when equation (1) is altered maintaining a constant stagnation pressure and temperature.

$$\text{Power} \propto \frac{\gamma^{1/2}}{M^{3/2}} \cdot \mu_0^2 \qquad (3)$$

Here, M is the molecular weight of the gas. In general, the viscosity coefficient and specific heat ratio decrease when the number of atoms constituting the molecules of the gas increases. Thus, the molecular weight increases and the number of atoms constituting the molecule often increase if a heavy gas is used, and the power required to drive the wind tunnel decreases according to equation (3). As an example, if Freon-12 were used,

the specific heat ratio would differ greatly from that of air, and its use would be inappropriate in tests of compressible flows [19].

Conversely, the stagnation temperature and the viscosity coefficient would change in the technique of reducing the stagnation temperature. Such changes could be approximated as follows.

$$\mu_0 = \mu_* \left(\frac{T_0}{T_*}\right)^{\omega} \quad 0.5 < \omega < 1 \qquad (4)$$

Here, μ_* and T_* are the viscosity coefficient and the temperature at that time. Using this equation, equation (1) could be transformed into the following.

$$\text{Power} \propto T_0^{1.5+2\omega} \qquad (5)$$

Thus, reduction in the stagnation temperature would be an effective means of requiring little power to drive the wind tunnel in order to produce a flow of prescribed mach number and Reynolds number. Figure 3.2 is used extensively to illustrate the effectiveness of this technique. This represents in graph form changes in various quantities at constant Mach number (1.0 in this case), constant stagnation pressure and constant wind tunnel size (cross sectional area of test section) when the stagnation temperature is reduced using the value when the stagnation temperature is 322°K as the standard.

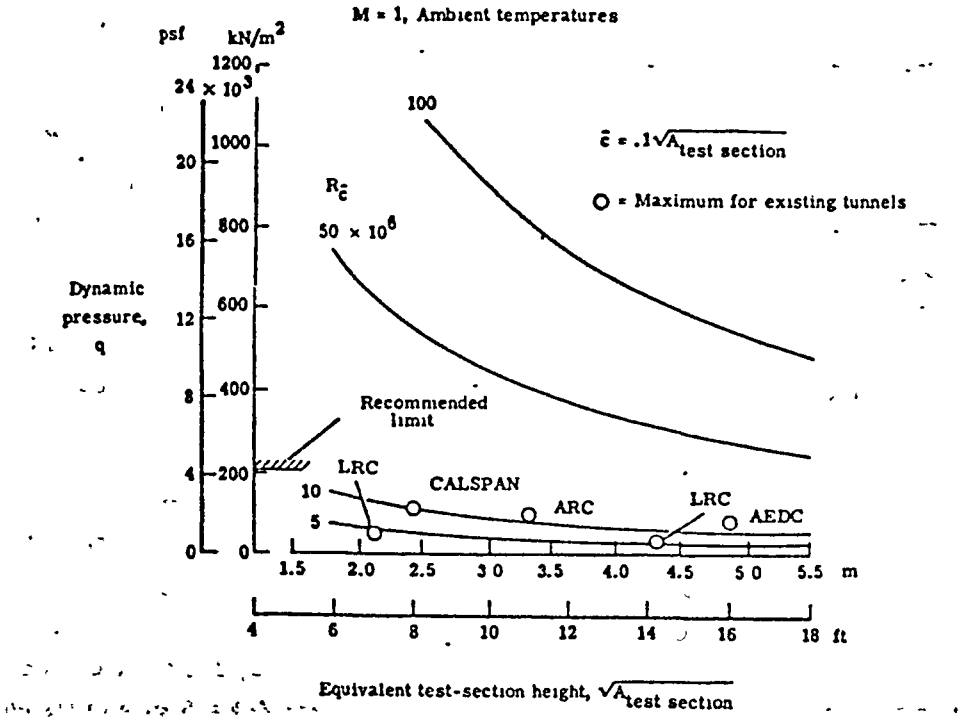

Figure 3.1 Dynamic pressure at various wind tunnel Reynolds numbers [9]

The Reynolds number $R_{\bar{c}}$ is expressed as follows.

$$R_{\bar{c}} = \frac{\rho M a \bar{c}}{\mu} \qquad (6)$$

Here, μ, ρ, a and M represent the viscosity coefficient of gas in the test section, the density, speed of sound and Mach number respectively. Because of the constant Mach number and constant size of the test section, M and $\bar{c}$ are constants. Figure 3.2 indicates that ρ increases rapidly when the stagnation temperature is reduced while μ and a decrease. However, μ

decreases faster than a. Thus, a/μ increases even if the stagnation temperature decreases. Thus, R^{-}_{c} generally increases when the stagnation temperature decreases. In this way, effective means of obtaining a flow of high Reynolds number at low power with reduction in the stagnation temperature are anticipated to produce various technical problems accompanying low temperatures, and practical application is not anticipated for a long time. /10

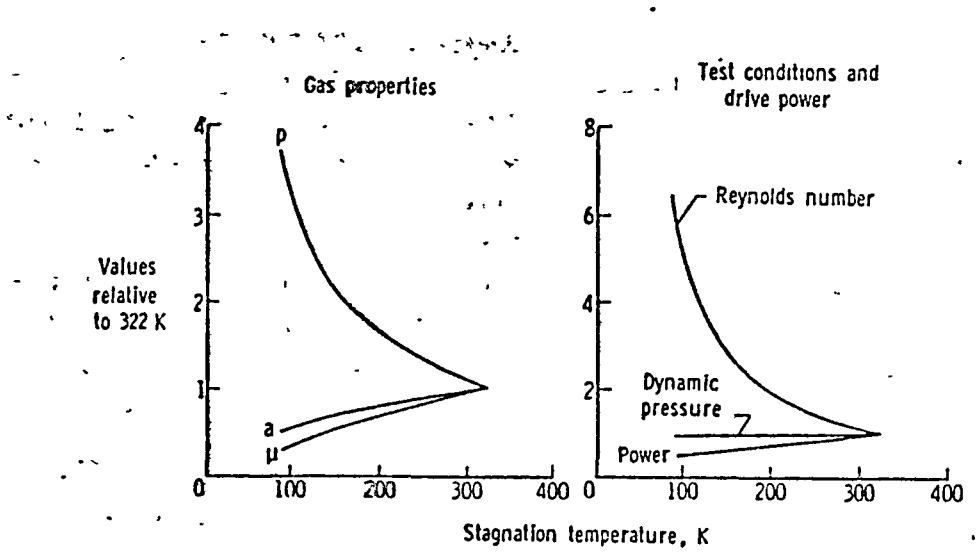

Figure 3.2 Effects of temperature reduction on gas properties, Reynolds number, dynamic pressure and wind tunnel power [17]. (uniform flow mach number = 1.0, constant stagnation pressure and size of the test section of the wind tunnel.)

The next chapter introduces several new types of wind tunnels, beginning with the cryogenic wind tunnel, which have been considered for high Reynolds number testing.

4. Wind Tunnel Models

4.1 Cryogenic Wind Tunnel

The method of sufficiently reducing the temperature of gas in a wind tunnel in order to acquire a flow with a high Reynolds number was proposed by R. Smelt in 1945 [17]. However, its implementation has been prevented until recently because of technical concerns involving wind tunnel operations at low temperatures. In 1971, research into this type of wind tunnel was conducted by NASA, and a small, low speed, cryogenic wind tunnel was produced (Figure 4.1) [24]. A small, transonic, cryogenic wind tunnel was then produced in 1973 (Figure 4.2) [25]. This is termed the 0.3 m transonic cryogenic wind tunnel. At present, a large transonic cryogenic wind tunnel with a test section having a 2.5 m x 2.5 m cross section is under construction (NTF) (Figure 4.3) [17,20]. Conversely, in Europe, a small transonic wind tunnel to begin operations in 1981 is under construction in Holland (PETW (Figure 4.4). A large transonic cryogenic wind tunnel with a test section of 1.95 m x 1.65 m is being planned based on the data obtained from this wind tunnel (Figure 4.5) [18,22]. A low speed, large cryogenic wind tunnel is under construction in Germany (Figure 4.6) [28]. A small transonic wind tunnel with a measurement cross section of 0.15 m x 0.35 m, which is scheduled to begin operations at the end of 1980, is under construction in France as well [21]. Completion of a low speed cryogenic wind tunnel of 0.5 m x 0.5 m at Tsukuba University in Japan is planned for 1981 [26], and a small, low speed, cryogenic wind tunnel is in operation at Tsukuba University (Figure 4.7) [27]. The wind tunnels mentioned above are all continuous types, but intermittent type cryogenic wind tunnels have also been contrived. The temperature reduction in the induction driven tunnel discussed in the next section has been promoted by ONERA of France (Figure 4.8 [33], while the Douglas Aircraft Co. in the United States has been promoting work on producing a cryogenic wind tunnel from a blowdown to

atmosphere type wind tunnel with a test section cross section of 1.2 m x 1.2 m. Operations are scheduled to begin in 1981 (Figure 4.9) [23].

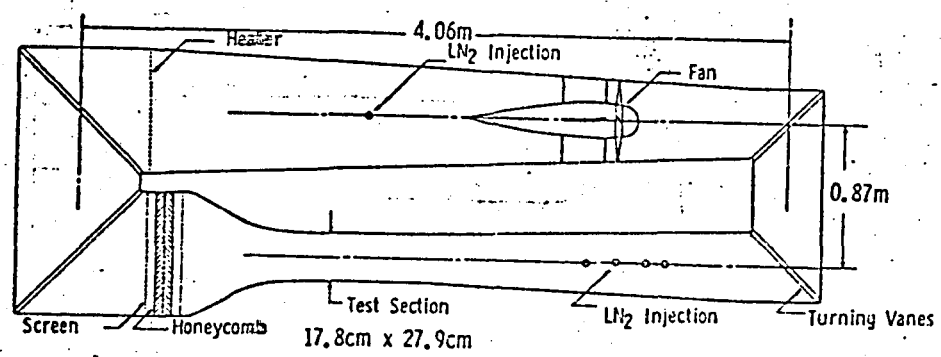

Figure 4.1 NASA Langley low speed cryogenic wind tunnel [8]

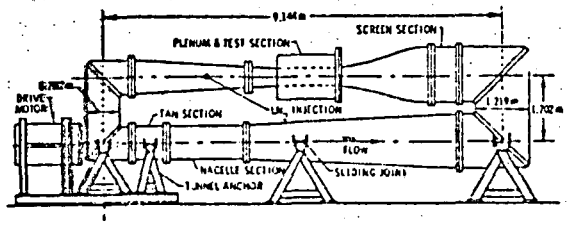

図4.2 0.3m transonic cryogenic wind tunnel[17)]

Figure 4.2 0.3 m transonic cryogenic wind tunnel [17]

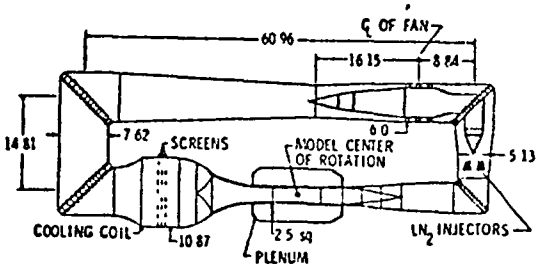

図4.3 National Transonic Facility[35] (NTF)

Figure 4.3 National Transonic Facility (NTF) [35]

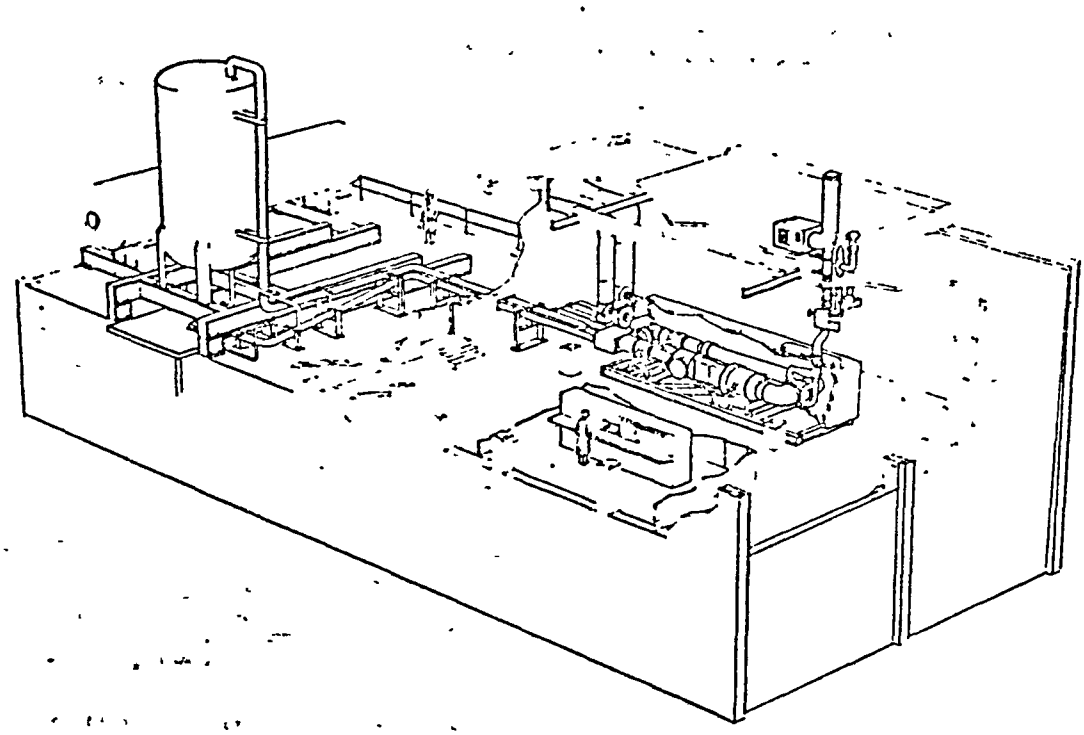

Figure 4.4 European small transonic cryogenic wind tunnel (PETW) [22]

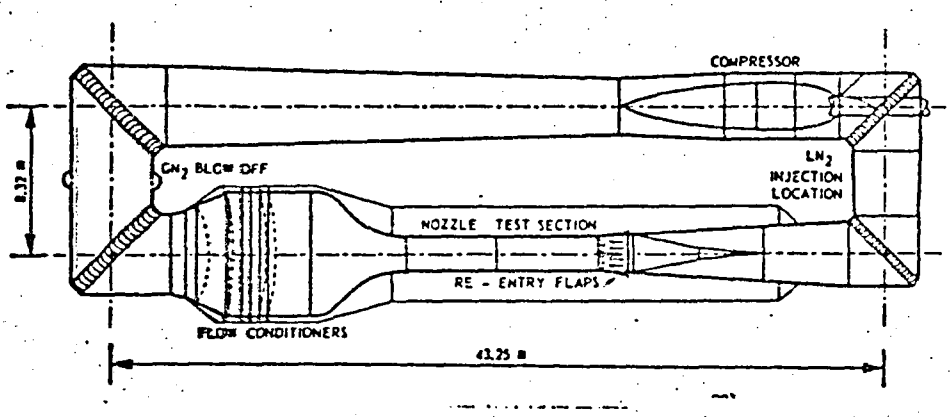

Figure 4.5 European transonic cryogenic wind tunnel (ETW) [22]

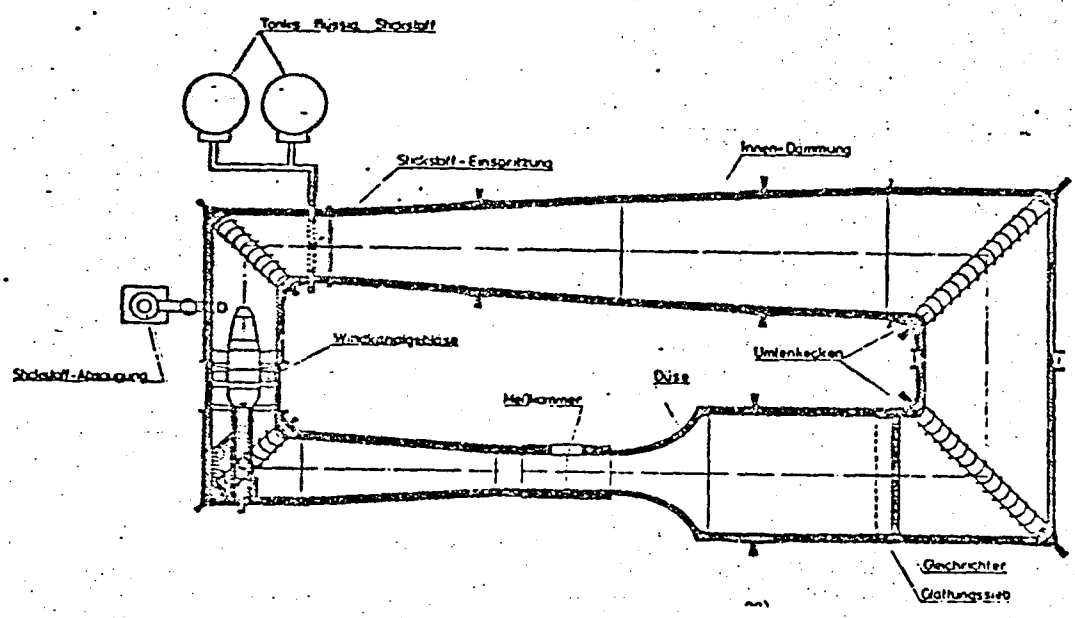

Figure 4.6 West German 2.4 m low speed cryogenic wind tunnel [28]

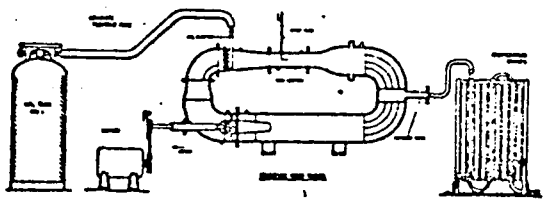

Figure 4.7 Tsukuba University small cryogenic wind tunnel with 10 cm x 10 cm test section [27]

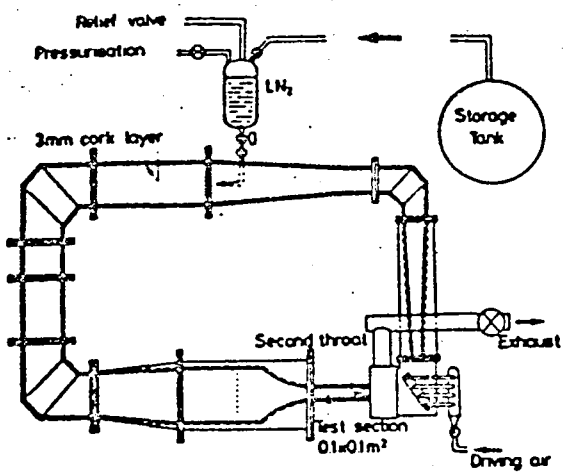

Figure 4.8 French transonic cryogenic wind tunnel (0.1 m x 0.1 m) (Induction Driven Type) [33]

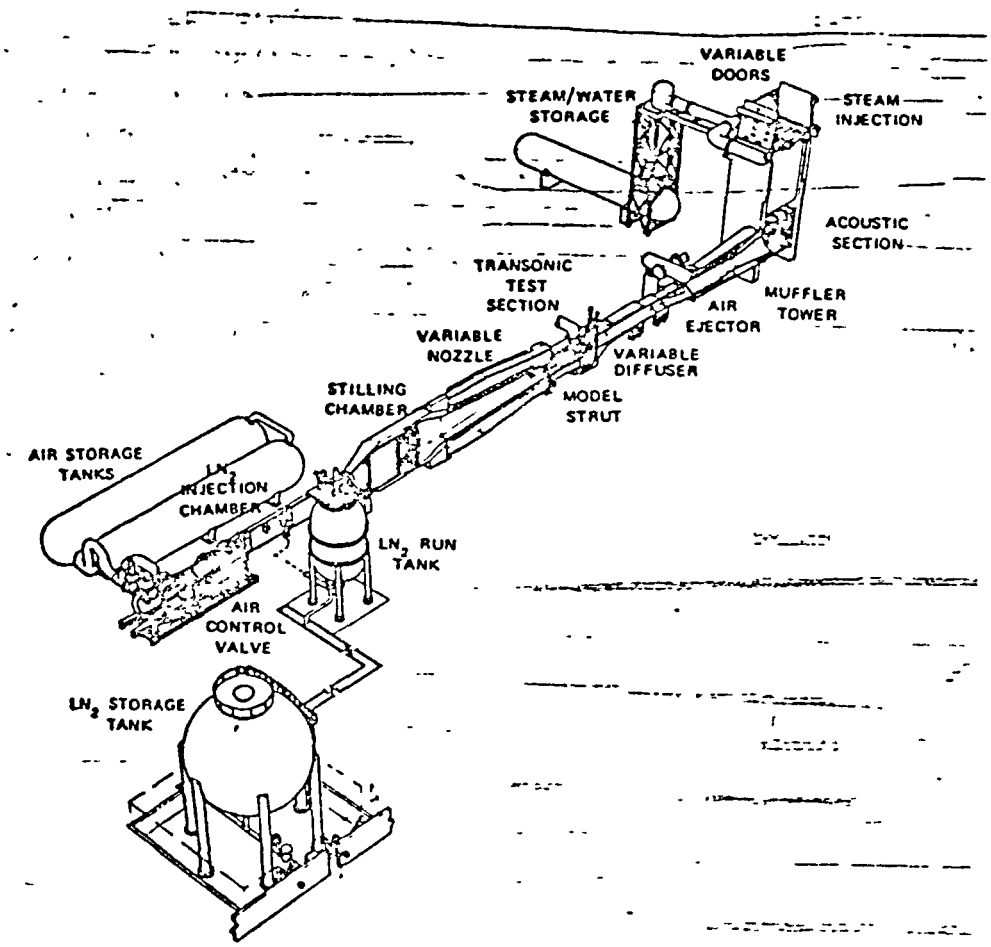

Figure 4.9 Douglas Aircraft Co. cryogenic ejection type wind tunnel [23] (4' x 4')

The advantages of a cryogenic wind tunnel are that the dynamic pressure of a uniform flow can be reduced in comparison to a normal temperature wind tunnel whose internal pressure has been raised to acquire a prescribed Mach number and Reynolds number, and that the energy demand to operate a wind tunnel can be reduced (Figure 4.10) [17]. In particular, the ability to

reduce the dynamic pressure is very desirable since it enables the strength of the model, of the "sting" supporting it and the capacity of the balance to be reduced. Furthermore, various /13
experiments are possible in a cryogenic wind tunnel since the temperature and pressure of the air in the wind tunnel can be controlled independently. For example, experiments are possible in which one of the three parameters of the Mach number, Reynolds number and dynamic pressure can be altered while the other two are held constant. By means of this, the true Mach number effect or Reynolds number effect can be determined (Figure 4.11). Conversely, the effect of gas diverging somewhat from ideal gas can begin to appear since the gas in the wind tunnel is reduced in temperature to the temperature near liquefaction. However, the influence of this effect on the test results has reportedly been buried in conventional test accuracy (Figures 4.12, 13) [17].

In order to reduce the temperature of the gas inside the cryogenic wind tunnel to the temperature near the liquefaction point and to maintain that temperature during operation, LN_2 identical with that in the wind tunnel, termed refrigerant, is continuously injected in the air duct. By means of this, the temperature of gas in the wind tunnel is maintained at a low point by the heat loss during evaporation of liquid. Of course, the mass of refrigerant injected in the air duct is exhausted at a suitable point in the air duct, and the pressure in the air duct is maintained at a constant. For this reason, operation of a continuous type cryogenic wind tunnel differs somewhat from that of a conventional wind tunnel. First, refrigerant is gradually injected in the air duct while the blower is operated at low speeds. At this time, the temperature of the gas exceeds the dew point of liquid in the wind tunnel circuit, and it is reduced near the limit at which measurement is possible by a dew-point thermometer (near -70°C). This is to prevent condensation of H_2O on the walls of the wind tunnel, on the wire mesh

and on the surface of the model from freezing. This operation is termed "purging". Next, the temperature of the gas in the wind tunnel is reduced to the stagnation temperature scheduled in the experiment while injecting large amounts of refrigerant. At this /14
time, excess gas is vented in proportion to the amount of refrigerant injected so that the pressure in the air duct does not rise. This operation is termed "cool-down". Next, the operating speed of the blower is raised, and experiments are conducted with the flow in the test section at the pre-set level while adjusting the amounts of refrigerant injected and of venting of gas in the air duct. The temperature of gas in the air duct would rise and be restored to the ambient temperature by the heat generated in the air duct and the heat invading from the walls if the supply of refrigerant were terminated and the blower operated at the end of the experiment. This operation is termed "warm-up". Next, air enters from the exhaust valve on the plenum side while gas in the air duct is vented from the exhaust valve on the stilling chamber side when the exhaust valves in the plenum and stilling chamber are opened and the blower is operated at low speed, thereby replacing the gas in the air duct with air. This operation is termed "reoxygenation". After this operation, the blower is completely shut down (Figure 4.14).

The differences in the cryogenic wind tunnel, in comparison to the continuous type wind tunnel which is operated at normal temperature, are that a refrigerant supply system and an exhaust system of gas in the air duct are added, and that the wind tunnel itself is thermally cut off from the atmosphere. In addition, liquid nitrogen is generally used as the refrigerant, and the gas in the air duct also is nitrogen gas as a result (Figure 4.15).

In the cryogenic wind tunnel, the gas in the air duct and the surrounding atmosphere must be thermally isolated by heat insulating material since the temperature of the gas in the wind

tunnel (approximately 100°K) is far lower than the temperature of the surrounding atmosphere (approximately 300°K). Methods of insulation include external insulation in which heat insulating material is affixed to the exterior of the wind tunnel body and internal insulation in which it is affixed to the walls inside the wind tunnel. Only the external insulation method is practical at present (Figure 4.16). In external insulation, the structural material itself is exposed to low temperatures, oxygen in the atmosphere invades the external heat insulating material and liquefies near the cold structures, resulting in local excesses of oxygen and the danger of fire [29], but this method is used extensively in small wind tunnels since it is simple. Conversely, when external insulation is used in large cryogenic wind tunnels, the structure itself must be cooled from normal temperature to low temperatures, and large amounts of refrigerant are required. This is also undesirable due to the deformation based on thermal change. For these reasons, internal insulation is employed in large wind tunnels under construction and being planned (Figure 4.17).

Furthermore, since the material exposed to gas in the wind tunnel is at normal temperature before operations of the wind tunnel begin and is then exposed to temperatures down to -200°C during operations, there are problems associated with contraction of material due to heat changes. Special consideration must be given to the struts of the model itself when the external insulation method especially is employed. Figure 4.18 illustrates an example of the struts used in the NASA 0.3 m temperature cryogenic wind tunnel. Moreover, special measures are required for the observation window (Figure 4.19), and special measures are required in the case of schlieren observation etc. Furthermore, the exhaust stack illustrated in figure 4.20 is essential to safely discharge nitrogen gas from the air duct to the atmosphere.

As stated above, various special devices are required in a cryogenic wind tunnel in comparison to a normal temperature wind tunnel due to operations at low temperatures, but when the NTF under construction at present by NASA, which has the capacity to reproduce on the ground the flow field of high Reynolds number produced around the large transports currently operating, is used, a flow field with a Reynolds number as in figure 4.21 would be achieved. Furthermore, the true Mach number effect, Reynolds number effect and effects due to changes in the dynamic pressure could be studied in wind tunnel experiments, and cryogenic wind tunnels have epochal capacities in terms of hydrodynamic research and of aircraft development.

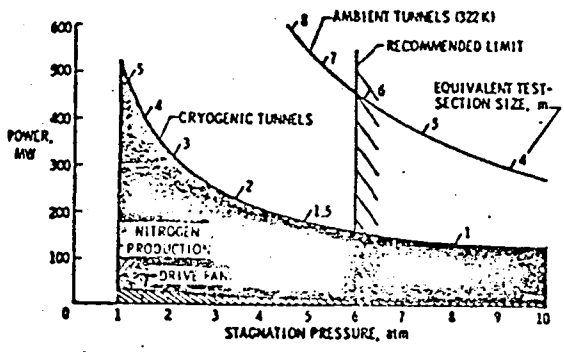

Figure 4.10 Power required to produce a flow field corresponding to $R_c = 50 \times 10^6$ at M = 1 in the test section [17]

/15

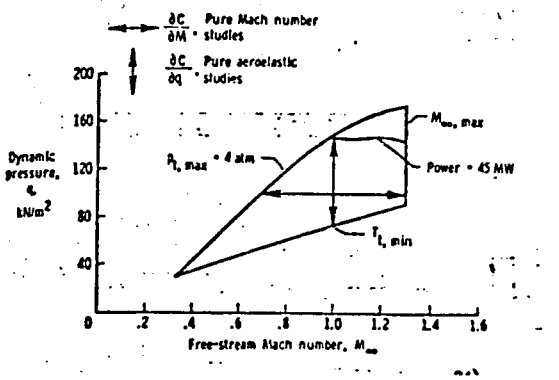

Figure 4.11 (a) Operation at constant Reynolds number [34]

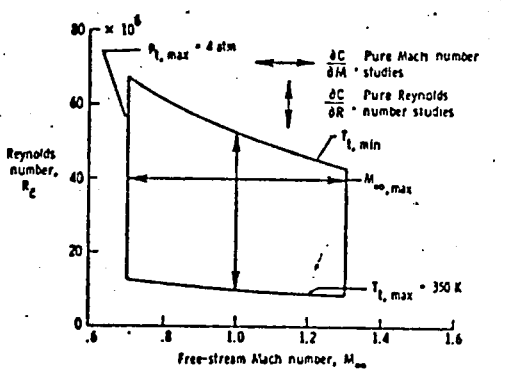

Figure 4.11 (b) Operation at constant dynamic pressure [34]

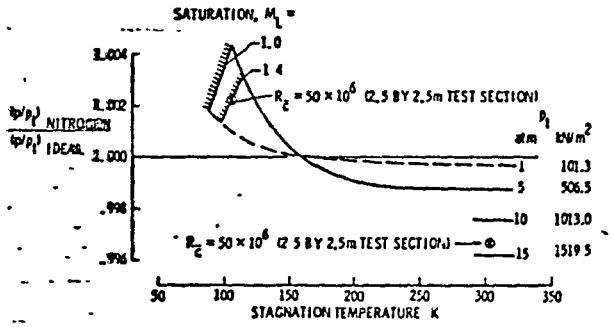

図 4.12 Isentropic expansion pressure ratio of nitrogen.[36]
Pressure ratio P/P_t ; $M_\infty = 1$.

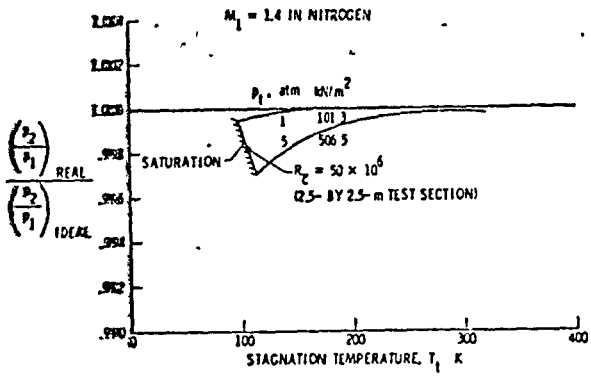

図 4.13 Normal shock pressure ratio in nitrogen.[36]

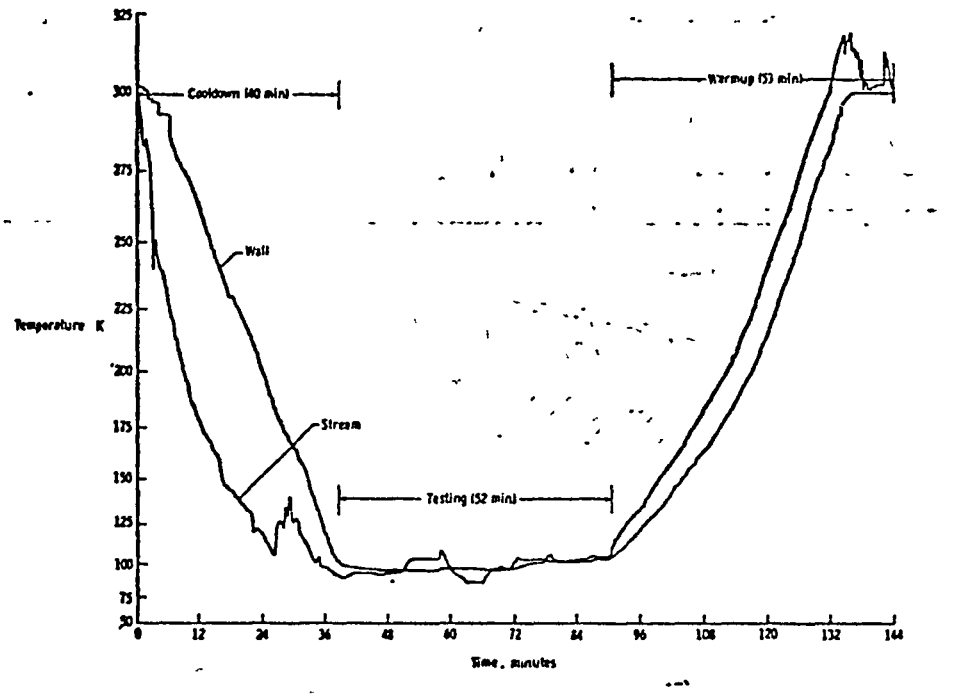

Figure 4.14 Temperature changes in flow and walls during operation [17]

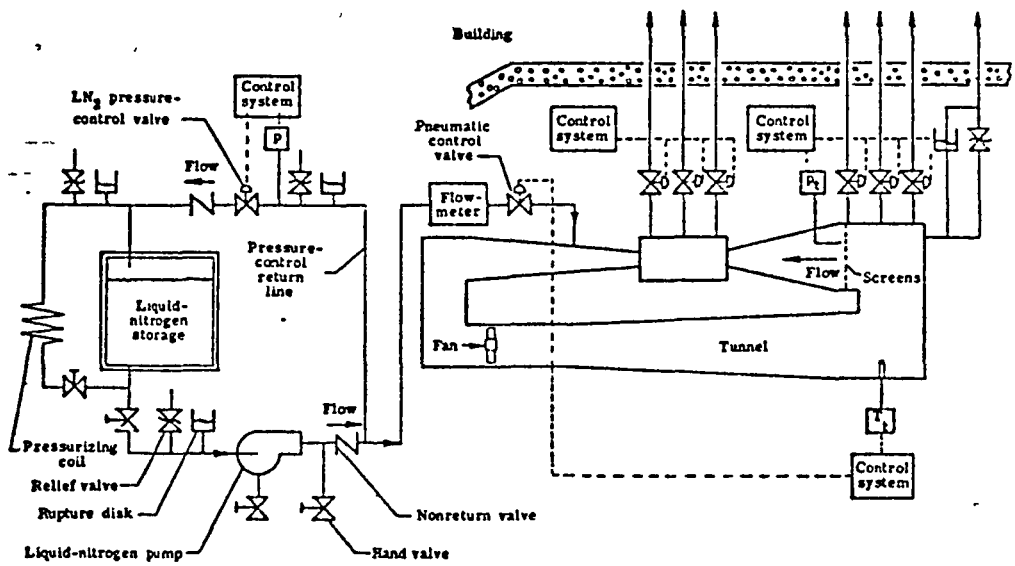

図4 15 NASA 0 3m Transonic Cryogenic Wind Tunnel

Figure 4.15 Figure of piping of supply of refrigerant (LN_2) and exhaust (GN_2) in NASA 0.3 m transonic cryogenic wind tunnel [17]

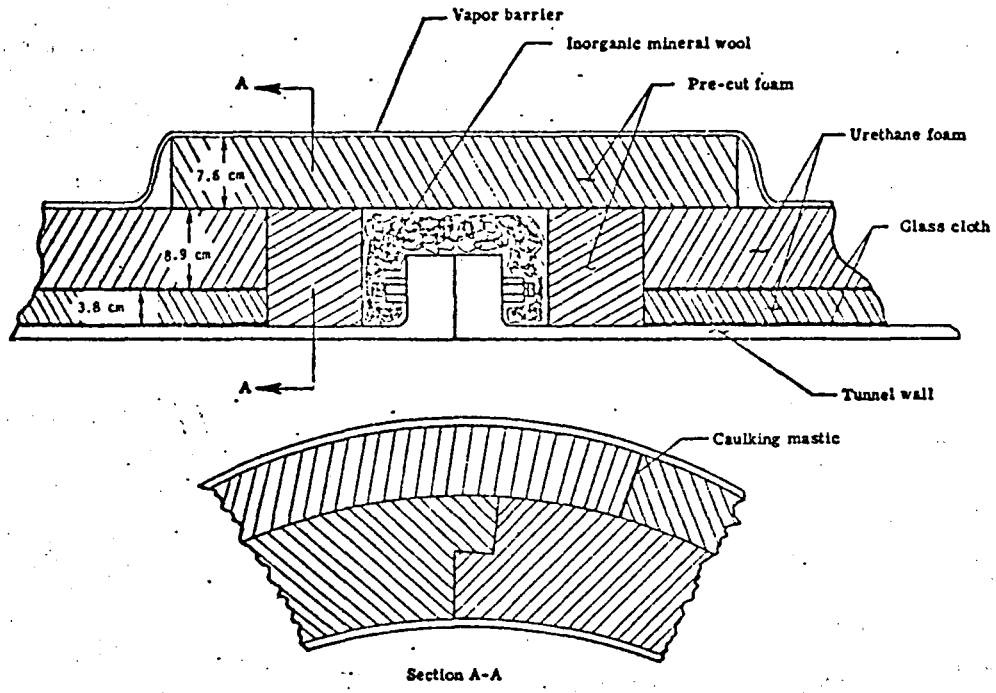

Figure 4.16 External insulation method [25]
[Original used on 0.3-m TCT]

/17

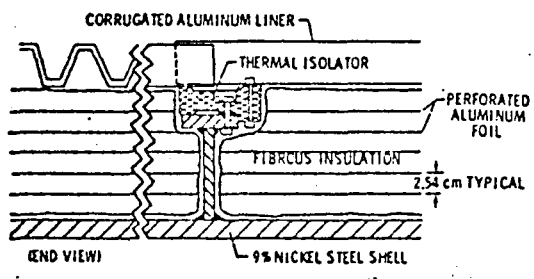

図4.17 内部断熱法[35]

Figure 4.17 Internal insulation method [35]

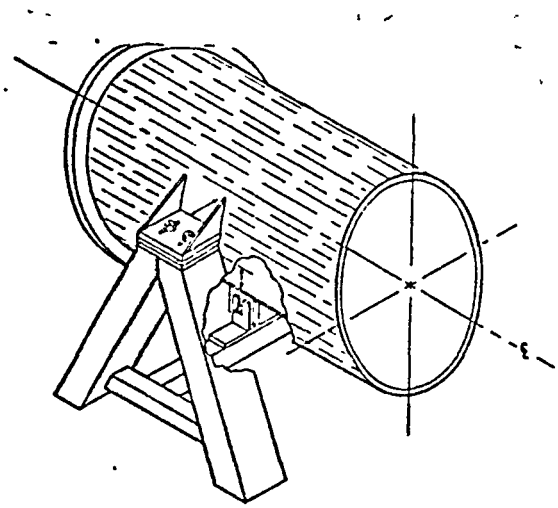

Figure 4.18 Struts of wind tunnel [25] [0.3-m TCT]

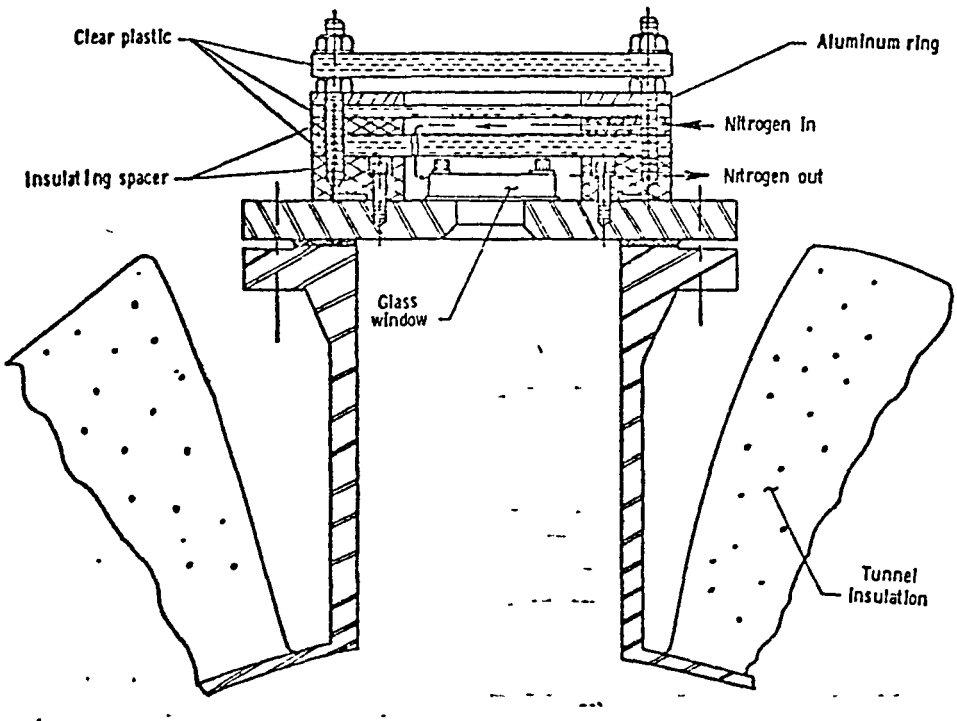

Figure 4.19 Wind for observation [25] [0.3-m TCT]

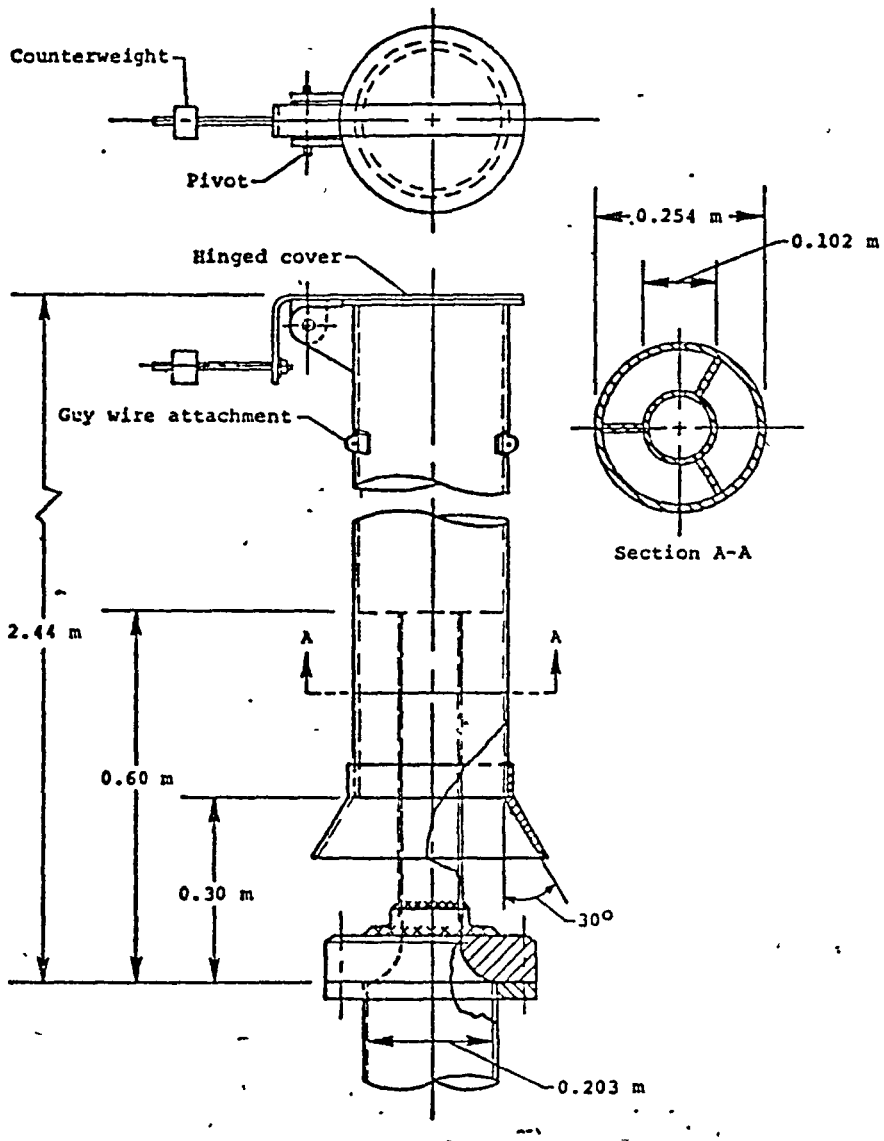

Figure 4.20 Exhaust stack [25] [0.3-m TCT]

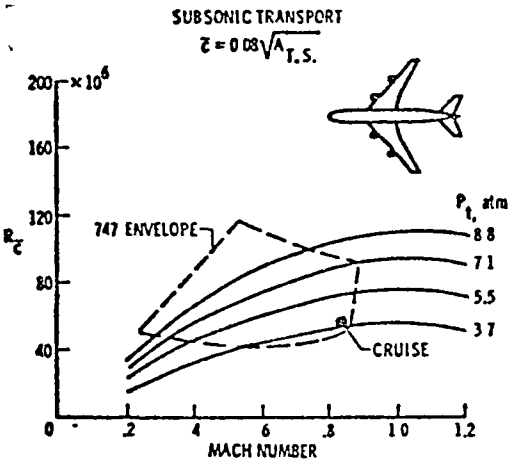

Figure 4.21 Range of mach number and Reynolds number produced by NTF [17]

4.2 Induction Driven Tunnel (IDT) /19

This type of high speed wind tunnel was devised before World War II [30]. The principle involves blowing a high speed jet in the air duct, inducing a flow in the test section in which the jet flows upward. The air duct is closed and the circulation type is employed for maximum utilization of the kinetic energy of the jet when considering a large, high-pressure test section. At this time, gas in the air duct corresponding to the mass of the jet blown into the air duct must, of course, be discharged into the atmosphere. Figure 4.22 illustrates the principle of this [31]. The fact that the site of discharge of gas in the air duct has a great effect on the operating efficiency of the wind tunnel when the flow in the test section exceeds a high subsonic rate has recently been clarified [31]. Figure 4.23 illustrates the improvements. Figure 4.24 illustrates the results of the improvements by comparing the efficiency of this type of wind tunnel constructed by NPL in the latter half of the 1940's with the efficiency of the NASA, Ames Research Institute wind tunnels. This type of large wind tunnel has materialized through

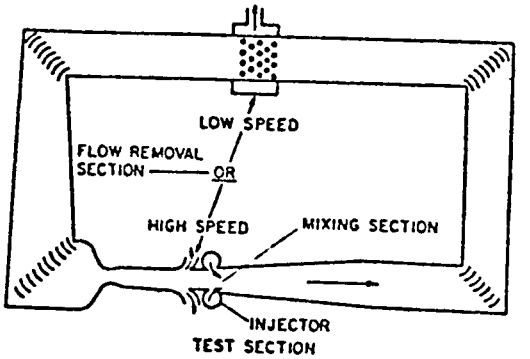

Figure 4.22 Induction Driven Tunnel [31]

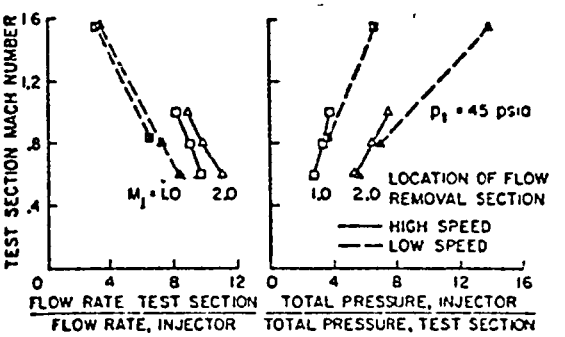

Figure 4.23 Differences in operating efficiency of wind tunnels based on location of flow removal section [31]

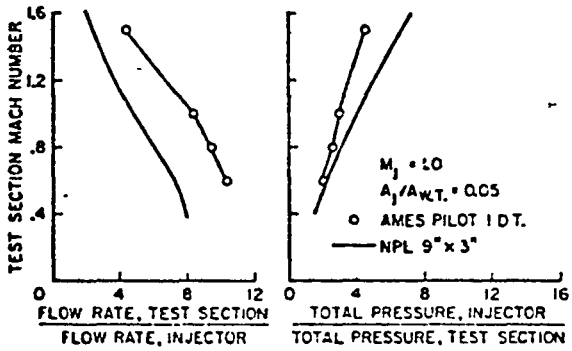

Figure 4.24 Comparison of NPL and IDT [31]

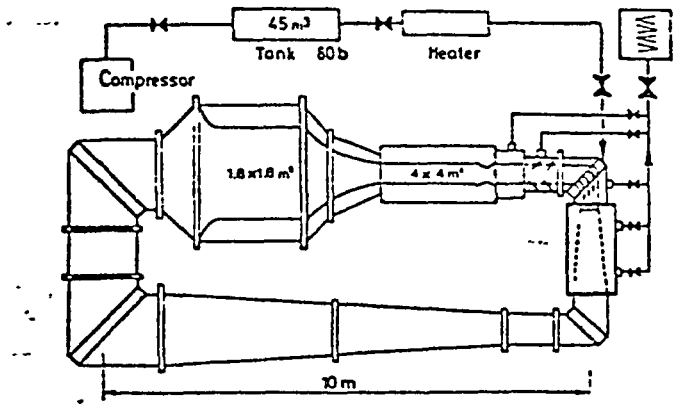

Figure 4.25 ONERA T2 wind tunnel [32]

such improvements in efficiency. This type of wind tunnel has been proposed as a large European wind tunnel of high Reynolds number by ONERA in France, and a 1/10 scale pilot wind tunnel has been constructed for research (T2) (Figure 4.25). This wind tunnel has a closed air duct and appears to be a continuous type wind tunnel, but the wind tunnel operation is terminated when the /20
tank supply a jet of gas through the air duct falls to a prescribed pressure. T2 is reported to have a running time of approximately 30 seconds [32]. This is a long operating time in comparison to the Ludwieg tube wind tunnel and the Evan wind tunnel which have been cited at the same time as candidates for the large European wind tunnel of high Reynolds number. This long operating time is an advantage of this type. Furthermore, research into conversion of the T'2 wind tunnel, which is a prototype T2 wind tunnel, into a cryogenic wind tunnel, has recently been carried out (Figure 4.8) [32].

4.3 Ludwieg Tube (LT)

The Ludwieg tube is a type of blowdown wind tunnel termed a tubular wind tunnel which was proposed by the German, Ludwieg in 1955. The Ludwieg tube is a strong candidate as a means of implementing test facilities with a high Reynolds number [7,37,38,39,40]. Its properties have been studied for several years at the National Aerospace Laboratory also [41,42,43,44,63].

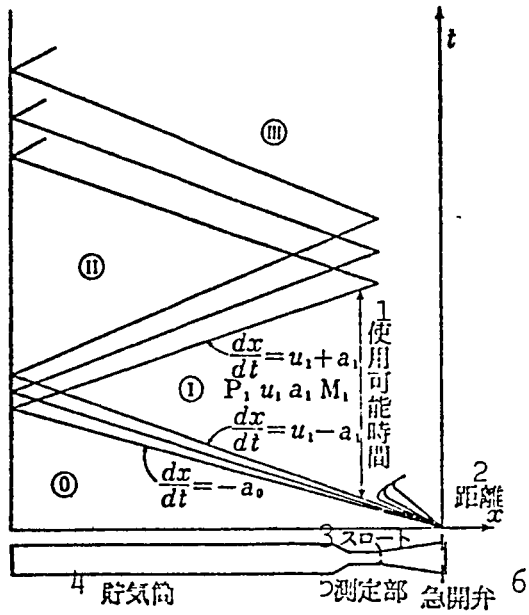

Figure 4.26 Principle of Ludwieg tube

1 usable time
2 distance
3 throat
4 charge tube
5 test section
6 quick opening valve

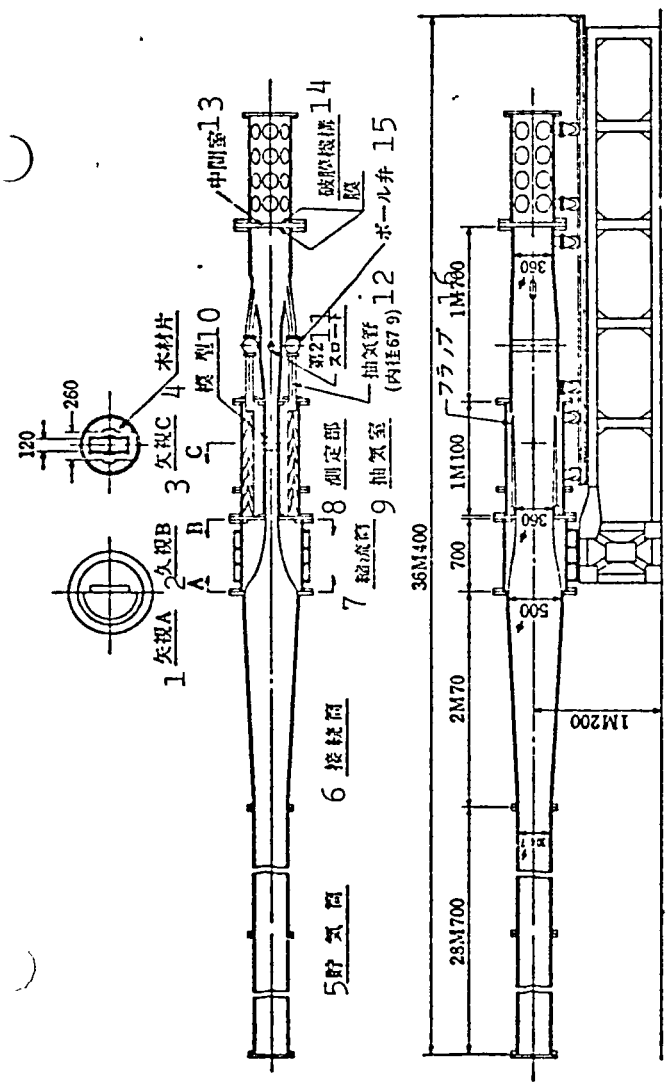

Figure 4.27 120 x 360 Ludwieg tube of National Aerospace Laboratory [42]

1 Section A
2 Section B
3 Section C
4 timber block
5 charge tube
6 connecting tube
7 contraction cone
8 test section
9 plenum chamber
10 model
11 second throat
12 plenum bleed tube - complete
13 intermediate chamber
14 rupture disk (structural membrane)
15 ball valve
16 flap

4.3.1 Structure and Actuation Principles

Figure 4.26 illustrates the structure and actuation principles. This figure illustrates the case of a subsonic flow in the test section. There is a long charge tube, as illustrated at the bottom of the figure, and a rapid opening valve at the bottom of the flow along with the usual constituent elements of a wind tunnel such as a throat, test section and contraction section at the bottom of the stream. The pressure regulation valve and settling chamber seen in the blowdown type wind tunnel are unnecessary upstream in the test section. When the rapid opening valve is opened after storage of high-pressure gas in the tube, the expansion wave begins to advance upstream from there, providing motion to the gas and initiating the discharge of gas. After valve opening, the speed of sound is reached in the throat section in a very short period of time, and passage of the expansion wave is subsequently impossible. The expansion wave /21
passing through the throat section before this is an expansion wave of finite width, and it continues passage through the test section and advances upstream through the long charge tube with a fixed cross sectional area. A constant state involving pressure, temperature, density and velocity is achieved in the region following the transit of the expansion wave, and that state persists until the expansion wave is reflected off the closed end of the charge tube and returns. This steady state ends with the arrival of the expansion wave, and after the wave is reflected again at the throat section and directed upstream, a separate, new steady state is achieved, with this process repeated until the pressure in the tube falls sufficiently, as illustrated in figure 4.26. High Reynolds number tests can be carried out due to high pressure in the tube and some cooling concept (7, 40), but the steady state used in the experiments is only the state achieved initially. The subsequent state is wasted discharge of gas so long as some means of recovery is not employed.

Figure 4.27 illustrates experiments using a small transonic Ludwieg tube. The test section in this figure is a rectangle 360 mm high and 120 mm wide. Since the charge tube cross section does not change to the cross sectional shape of the test section merely through smooth contraction, contraction occurs after expansion once. Furthermore, timber blocks are filled in the plenum chamber to prevent the starting time from becoming excessive. This rupture disk structure is a double diaphragm type.

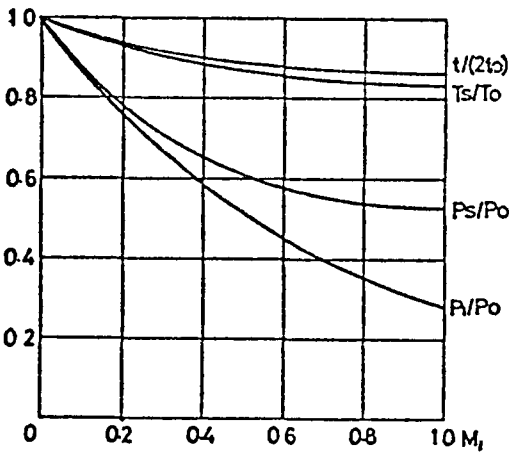

Figure 4.28 Differences in recovery rates based on mach number M_1 in charge tube and changes in duration

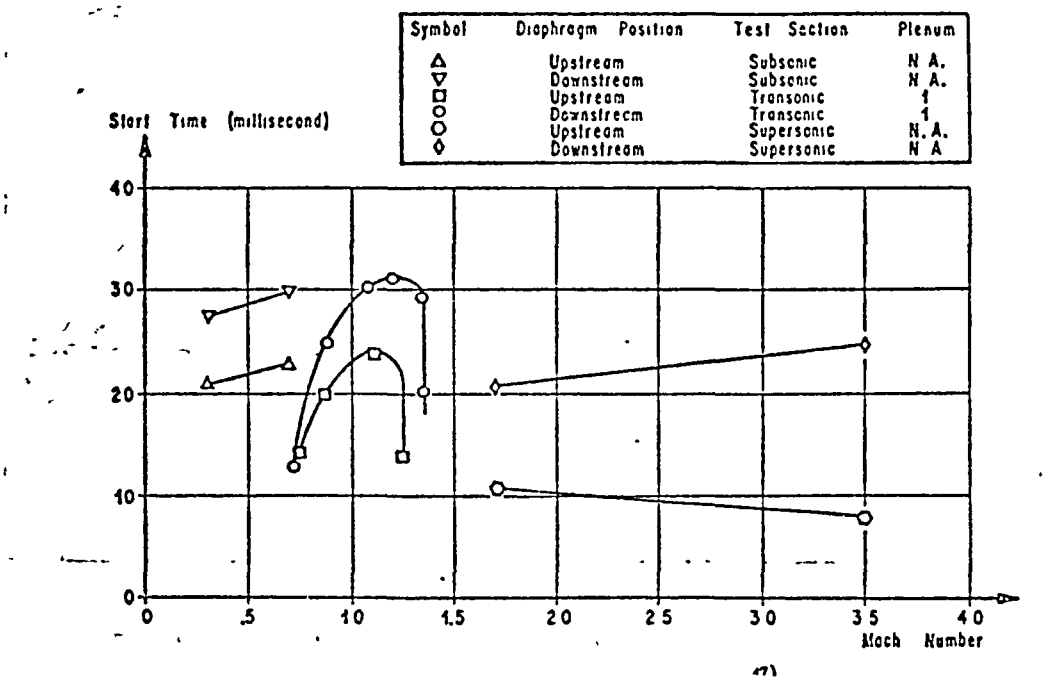

Figure 4.29 Starting time of Ludwieg tube [47]

4.3.2 Properties, Features

The properties of the flow obtained theoretically and the experiment results are summarized below.

i) The state at the stagnation point in the steady state obtained initially after passage of the expansion wave differs from the air storage state [45]. It depends on the Mach number (Mach number of the flow in the charge tube after passage of the expansion wave) of the charge tube, and is illustrated in figure 4.28. In the figure, P represents the pressure, T the temperature, ρ the density, the subscript 0 the air storage state while the subscript s represents the state at the stagnation point in the steady state.

t is the duration of the steady state in the ideal case, and /22
it is somewhat dependent on the Mach number of the charge tube. It is represented in the figure in the ratio to 2 t_0, the time for reciprocation through the charge tube at the speed of sound.

ii) The duration of the steady state is short, usually on the order of 10^{-1} seconds. Since the duration of the steady state is determined by the length of the charge tube (dependent somewhat on the Mach number in the charge tube), a very long charge tube would be required to obtain a long duration, and one which is 2 km in length is being planned [46]. A short experimental period is undesirable in wind tunnels for the development of aircraft requiring the production of large amounts of data. An improved method is ECT discussed subsequently.

iii) The starting time until acquisition of a steady state has been studied experimentally [47,48] and in calculations [43,49,50]. Calculations have also been carried out in cases of porous walls as in the transonic test section. The starting time is affected by the Mach number of the test section, and the longest starting time is required to obtain a transonic flow. Figure 4.29 illustrates an experimental example based on three types of test sections at subsonic, transonic and supersonic speeds. The starting time is shorter when a rapid opening valve (a film in this case) is present upstream in the test section, however, it influences the gas and model.

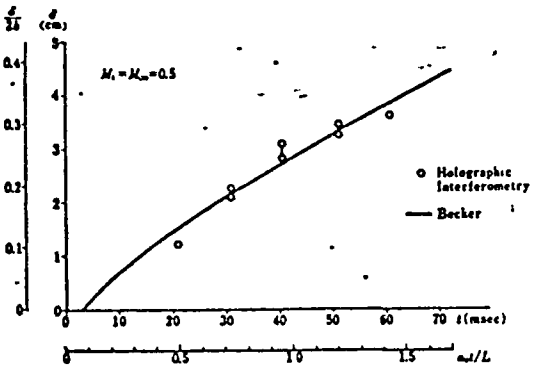

Figure 4.30 Development of boundary layer in charge tube [44]

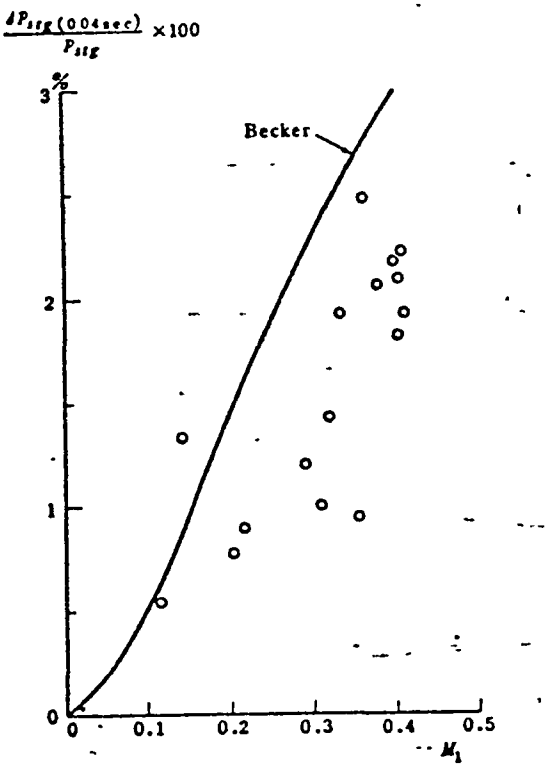

Figure 4.31 Changes in time of stagnation pressure based on charge tube mach number [41]

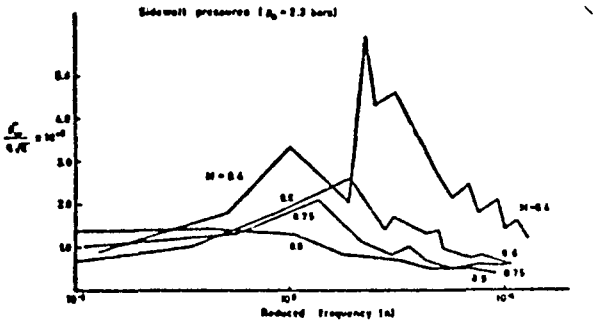

(a) 測定部壁圧の変動

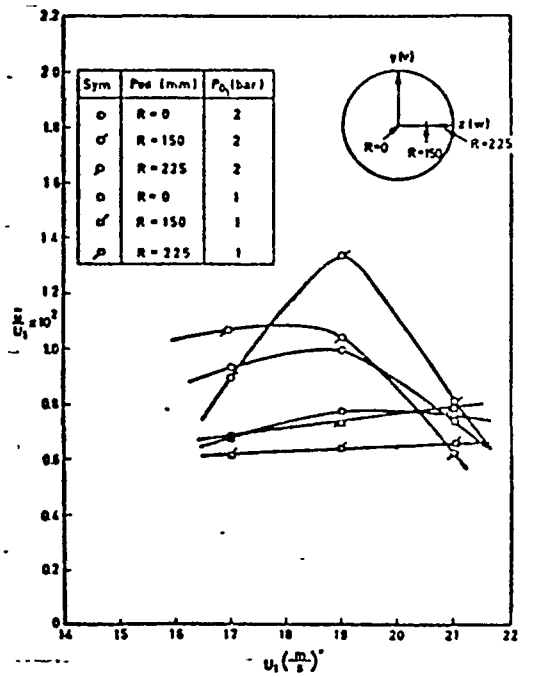

(b) 集合胴部の速度変動

Figure 4.32 Disturbance of flow in Ludwieg tube [54]
(a) fluctuations in sidewall pressure in test section
(b) fluctuations in rate of collection body

iv) The steadiness of the steady state is not very good /2
This is because the so-called free mode is used without any devices such as valves which control steadiness, in contrast to the blowdown type wind tunnel. The cause of loss of steadiness is the development of the boundary layer [51,52,53]. For example, the boundary layer in the charge tube changes while intensely dependent on the Mach number M_1 of the charge tube, as illustrated in figure 4.30, and chronological changes in the stagnation pressure occur due to this, as illustrated in figure 4.31.

The most serious problem is steadiness in the test section, and there are also cases of change in the Mach number in a very short time during tests [42].

Turbulence in the air flow is an important property in test equipment with a high Reynolds number. Since there is no valve or blower etc. upstream in the test section in the Ludwieg tube, turbulence level is believed to be slight. In comparison test results involving disturbance of the flow through pilot wind tunnels such as the ECT with a similar structure (refer to section 4.4) or the induction driven tunnel (IDT) discussed in section 4.2 [54], the amount of fluctuation of static pressure in the test section is greater than with other types. Figure 4.32 (a) is a plot with the ordinate being the rms value of the amount of fluctuation in the sidewall pressure of the test section divided by the square root of the relative zone width, which changes non-dimensionally with dynamic pressure, while the abscissa is non-dimensional frequency. Figure 4.32 (b) is a plot of the vertical velocity fluctuation of the collection body upstream in the test section.

v) The energy loss is great. As stated previously, the high-pressure air stored in the tube which can be used in the tests is the air required to maintain the steady state initially obtained, and the air whose discharge continues after termination of that state is wasted. Immediate closure of the rapid opening valve after termination of the initial steady state, or installation of a pressure recovery tube of identical length as that of the charge tube at the downstream end have been considered as proposed improvements to recover energy in the form of pressure. The energy utilization rate of 4.5% in the absence of such a recovery tube can be raised to 29.2% through its use [46].

vi) The structure is very simple. The number of devices is less than with other types of wind tunnels, and the rapid opening valve is the only complex constituent element. Consequently, construction is also easy, and the frequency of breakdowns is low while repairs are easy.

4.3.3 Some Examples

A comparatively large Ludwieg tube is at the NASA Marshall Space Center. The test section has a diameter of 813 mm (32 inches) while the charge tube has a diameter of 1.32 m (52 inches) and length of 119 m (390 feet) [39]. It is capable of testing at Mach number of 0.2 to 2.0. There is an experimental time lag of 0.35 to 0.45 seconds in the transonic region, and experimental results have been issued [55].

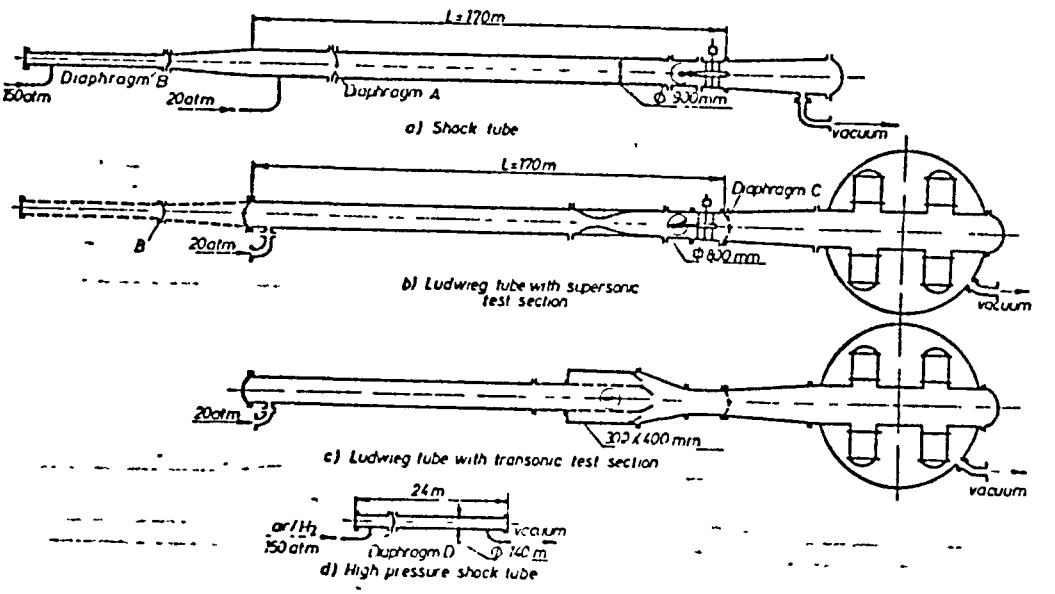

Figure 4.33 Ludwieg tubes of three sonic speeds at Rumanian NISTC [56].

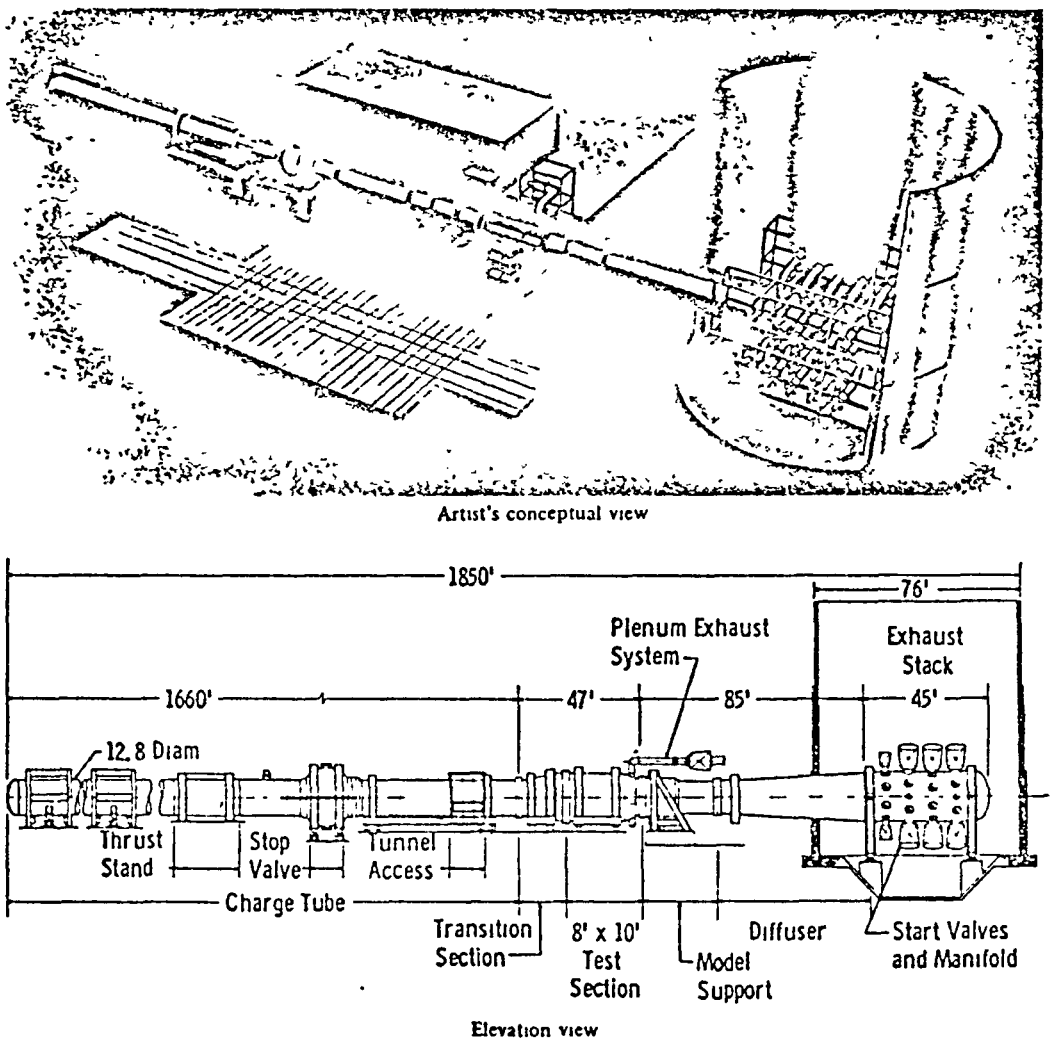

Figure 4.34 (a) AEDC proposed large Ludwieg tube [59]

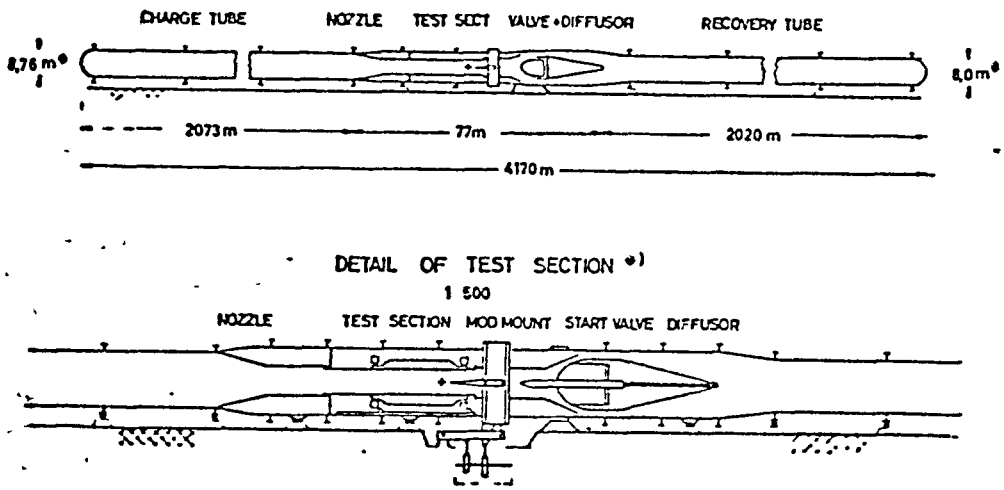

Figure 4.34 (b) Large Ludwieg tube fitted with recovery tube (top) and test section (bottom) [46]

The Ludwieg tube recently reported by the Rumanian Science and Technology Center (NISTC) is large. There are three types of test sections for subsonic use, supersonic use and transonic use. The test section is 300 mm x 400 mm during transonic experiments. The charge tube has a diameter of 900 mm and length of 170 mm /25 (refer to figure 4.33) [56].

In addition, a Ludwieg tube with a charge tube 700 mm in diameter and 75 m in length is under construction at the Chinese Institute of Science, Dynamic Research Center, and there are similar plans underway in India [58].

The very large Ludwieg tube planned by AEDC in 1971 with a 2.4 m x 3.0 m (8' x 10 ') test section and a charge tube with a 3.9 m (12.8') diameter and 500 m (1,660') length would have been capable of transonic testing at a Reynolds number of 40×10^6 [7,59]. While illustrated in figure 4.34 (a), it was not constructed due to budgetary concerns.

In Europe as well, AGARD has planned construction of a large transonic wind tunnel, and the Ludwieg tube fitted with a recovery tube was presented in 1972 as a candidate [15,46]. This would have a total length of 4.17 km, as illustrated in figure 4.34 (b), but it appears to have been cancelled in the project stage.

The Ludwieg tube has a simple structure, as indicated previously, and is easily capable of testing ranging from transonic to supersonic testing, and has been used [60], but as a large facility of which amount of energy consumption and data production are important, Ludwieg tube is not a good candidate. Rather, it should be used as a simple test device.

4.4 Evans Clean Tunnel (ECT/RTT)

The Evans Clean Tunnel (ECT) was proposed in 1971 by Evans [62]. Its principle is illustrated in figure 4.35. The composition of the entire wind tunnel is virtually identical with that of the LT discussed in section 4.3, but the upstream edge of the charge tube has a piston installed rather than a sealed edge. The plug valve at the downstream edge of the diffusor is closed, and the entire wind tunnel is charged to a certain pressure. Next, an expansion wave is propagated when the plug valve is rapidly opened, and air within the wind tunnel begins to be discharged. When choking of the flow occurs in the throat section, an expansion wave of finite wavelength is propagated upstream in the charge tube. The aforementioned is absolutely identical with the principle of the LT. The piston pushes from the instant that the tip of the expansion wave reaches the upstream edge of the charge tube (piston surface), generating a compression wave and completely eliminating the reflected wave. This is the principle of the Evans Clean Tunnel. Figure 4.36 illustrates a wave propagation figure.

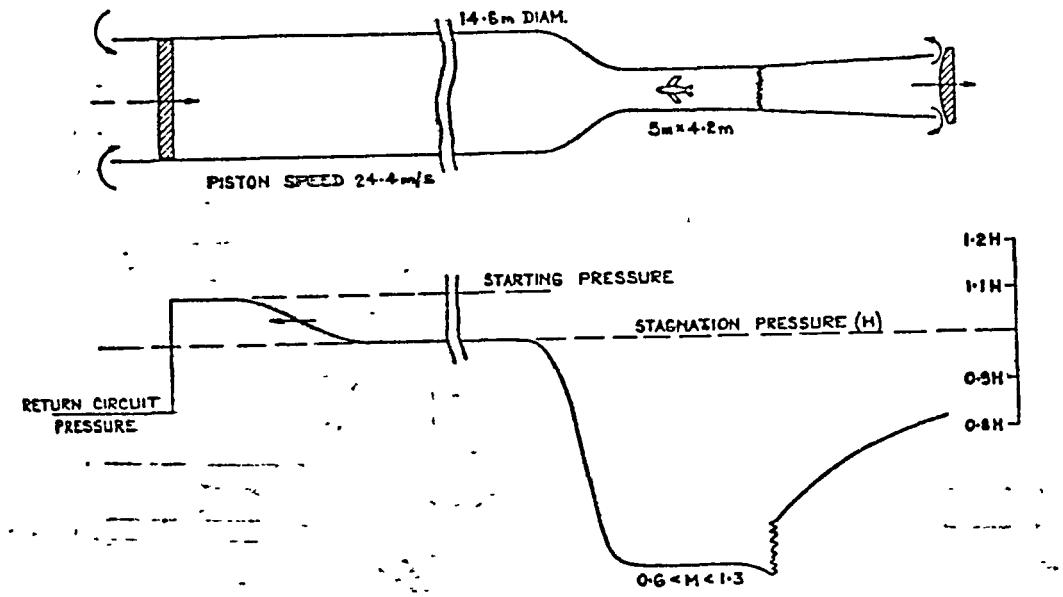

Figure 4.35 Principle of Evans Clean Tunnel [62]

The locus of the piston which completely eliminates the reflected wave is equal to the locus of the fluid particles accelerated by the incident expansion wave. In this case, either the locus of the piston is prepared so as to match the waveform of the given expansion wave, or the piston locus is given and the waveform of the expansion wave is prepared so as to match it.

After the tail of the expansion wave reaches the surface of /26
the piston, the piston functions at a constant rate, and a steady flow is maintained in the test section until the piston reaches the downstream edge of the charge tube, specifically the nozzle inlet. The duration of this steady flow is determined by the length of the charge tube in the case of LT, while it is determined by the volume of the charge tube in this case. Figure 4.37 illustrates a simple comparison of the durations of the ECT and LT. The duration of ECT is 5.8 to 2.6 times longer than that of LT since the charge tube Mach number M_1 is usually 0.1 to 0.3.

Operation of the ECT is efficient in terms of energy and air mass (Figure 4.38)

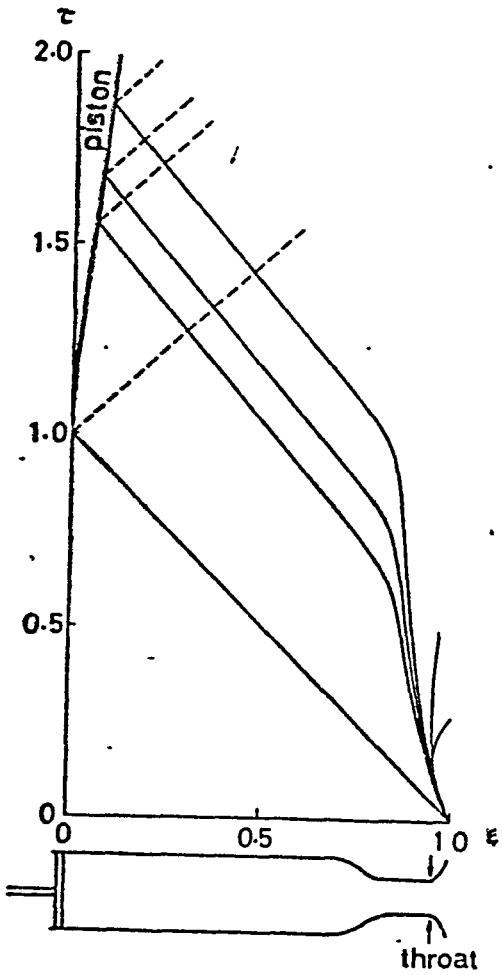

Figure 4.36 Wave propagation figure

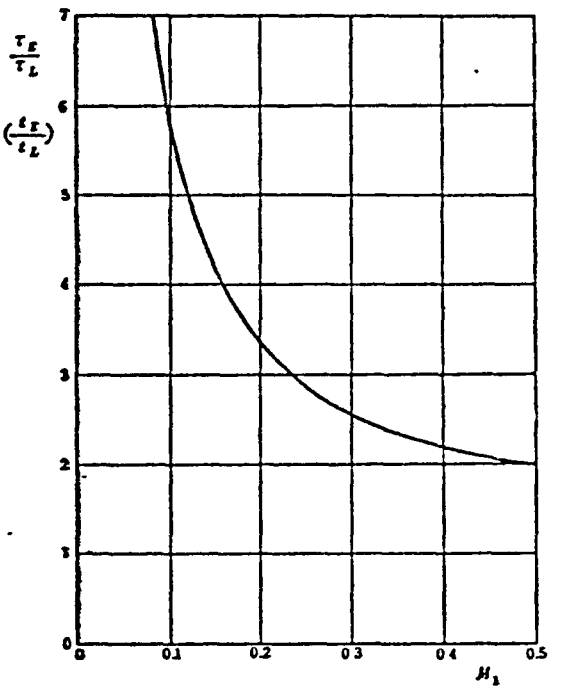

Figure 4.37 Possible time extension [63]

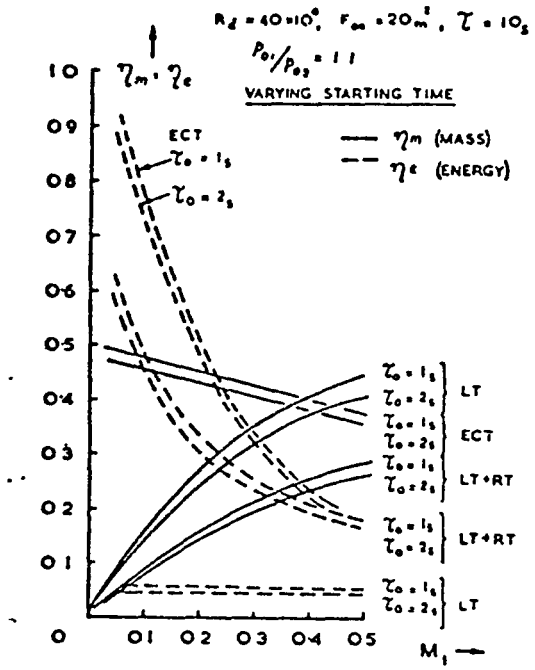

Figure 4.38 Comparison of efficiency [65] (RT: recovery tube)

Experiments were carried out using the device illustrated in figure 4.39 to illustrate the utility of the wave elimination which is the essential feature of ECT [64,65]. The piston is operated solely by the pressure differential acting on it without specific control of piston movement. The compression wave produced by movement of the piston is measured, and a cam plate is designed to produce a waveform of the expansion wave to match this.

Figure 4.40 illustrates the results of wave elimination. The optimum timing of piston release is the instant when the tip of the expansion wave reaches the piston surface. Even when wave /27

elimination is best, pressure fluctuation of 11% (6.4 mmHg) remains. This fluctuation is due to piston overshoot.

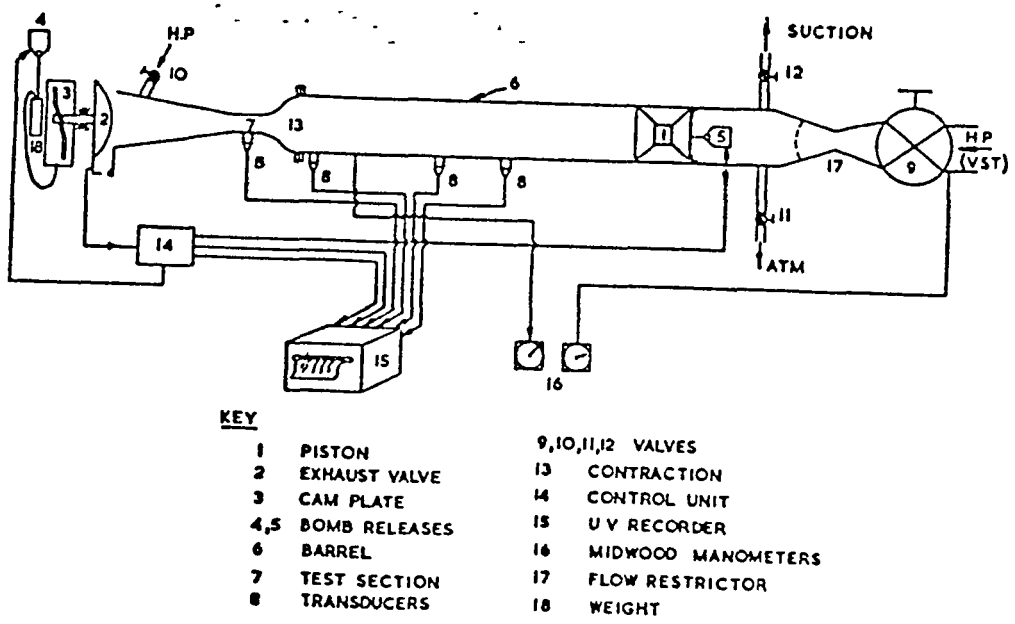

Figure 4.39 Conceptual figure of test device [65]

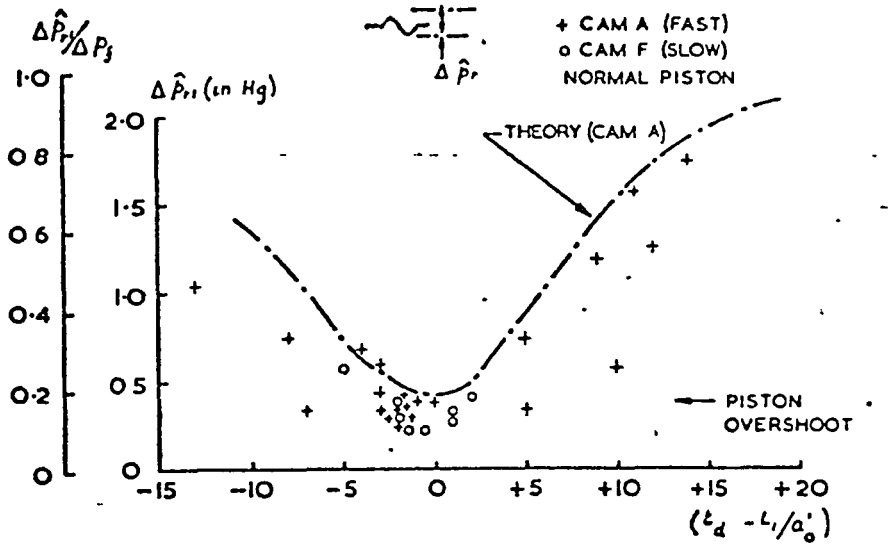

Figure 4.40 Test results of wave elimination [65]

In addition, experiments were carried out using the device approximating the proposed example illustrated after the piston drive method (Figure 4.41) [66]. In this drive method, four wire ropes from the center of the main piston are individually linked with small drive pistons via pulleys. Thus, acceleration of the main piston assists the air actuator.

Figure 4.42 illustrates the results of wave elimination. The optimum case is achieved through the cam designed point, and the mean square value of fluctuation of the stagnation pressure is 0.26%. This is a marked improvement in comparison to the previous experiments. Numerous aerodynamic tests have been conducted in this wind tunnel. Figure 4.43 illustrates a proposed example of design to conform to the requirements of the LaWs group. The compression flow ratio was 8 while the test section was 4.86 m x 4 m. The charge tube was charged to 6.6 atmospheres pressure in order to achieve a stagnation pressure of 6 atmospheres when the mach number in the test section is 0.9. The valves used were plug valves or digital valves. /2!

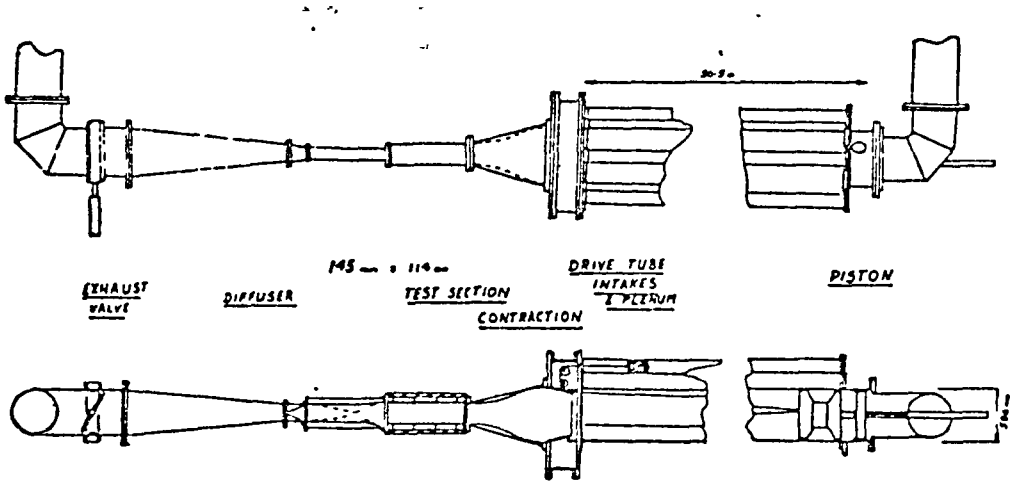

Figure 4.41 ECT pilot wind tunnel [65]

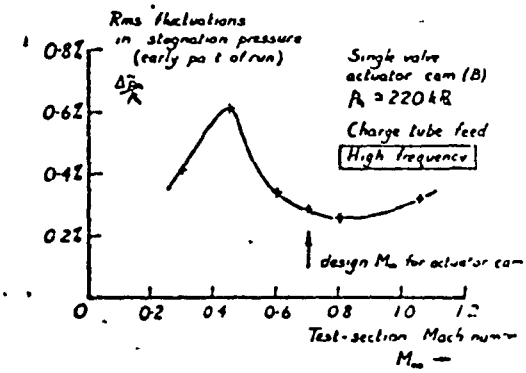

Figure 4.42 Results of wave elimination in pilot wind tunnel [66]

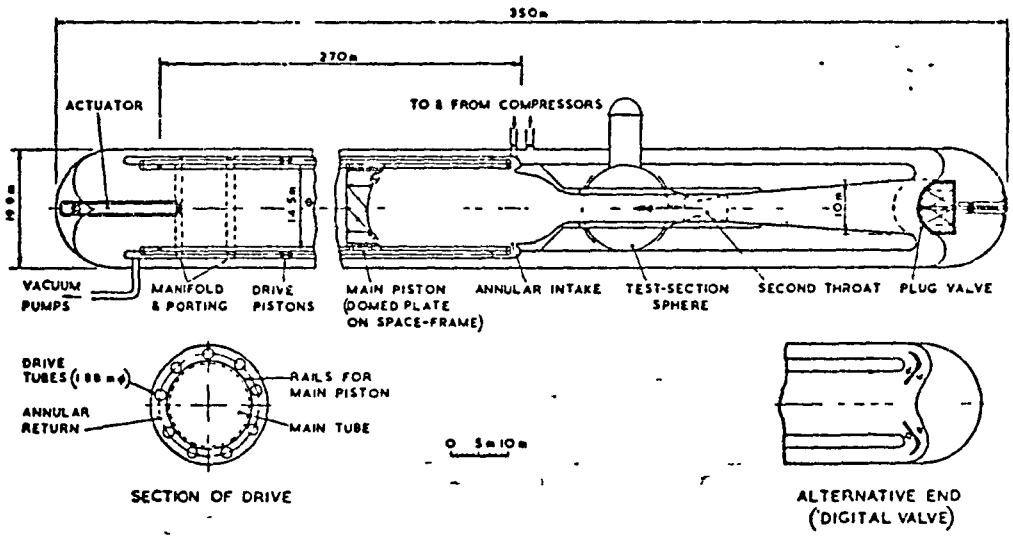

Figure 4.43 ECT transonic wind tunnel [65]

Figure 4.44 illustrates the project at RAE Bedford. In the full-scale model, the Reynolds number could be 16 x 10^6, and the test section is 1.26 m x 1.12 m.

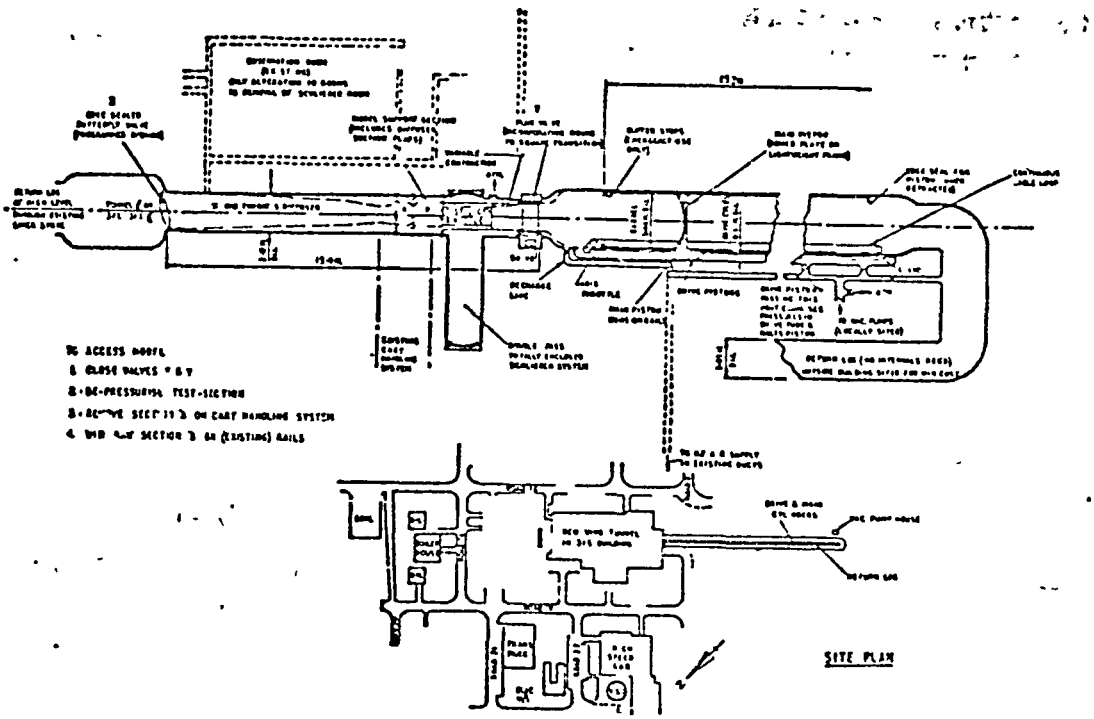

Figure 4.44 RAE-Bedford proposal [10]

The greatest problem in operation of the ECT is control of operation of the main piston or of the aperture of the exhaust valve so as to completely eliminate the wave. The control system is complex since these methods of control vary depending on the Mach number of the uniform flow or on the test model. Because of this, the method in which the solid piston is replaced by fluid (Reservoir and Tube Tunnel or RTT) has been considered [67]. As illustrated in figure 4.45, this method requires a reservoir and orifice at the tip upstream in the charge tube, and it is used as a method of increasing the duration of steady flow in shock wind tunnels [68]. The optimum aperture ratio of the orifice is a function of the Mach number of the charge tube [63]. In the RTT method, the case in which the aperture ratio of the orifice is altered periodically [71] is superior to the case in which it is

constant [69, 70]. In this case, the orifice control system is simpler than the piston control system of ECT. However, RTT is less efficient than ECT in terms of mass by the portion of air mass charged in the reservoir.

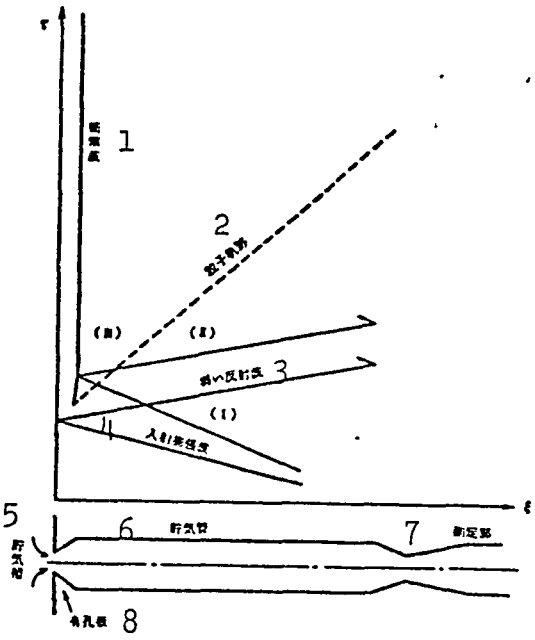

Figure 4.45 Figure of ξ and τ at optimum aperture ratio [63]

1 shock plate
2 particle locus
3 weak reflected wave
4 incident expansion wave
5 reservoir
6 charge tube
7 test section
8 orifice

4.5 Wind Tunnels using Hydraulic Power etc. /30

4.5.1 Concepts of Hydraulic Power Use and Energy to Drive Wind Tunnels

Enormous amounts of energy are required to drive wind tunnels in high Reynolds number tests, as explained in chapter 3. Cryogenic wind tunnels reduce the energy demand through reduction of the wind speed, but other wind tunnels store high-pressure air and achieve great air flows ($\because 1/2 \cdot \rho v^3$) for short periods of time through air release. However, when storing energy as high-pressure air, the easiest storage and best efficiency are obtained at high pressure, low capacity. Since the flow required for transonic wind tunnels is a flow of low pressure ratio and large flow rate, the high-pressure air storage method poses defects. This is different from the case of supersonic wind tunnels and ultra-sonic wind tunnels.

One compromise proposal has been the method in which a gas turbine is operated without direct utilization of released air. The axial flow blower linked to this turbine would then be driven for several minutes to serve as the source of power for the circulation type wind tunnel. Of course, use of a combustion device to produce high temperature air in the fan of a so-called jet engine which spins a turbine involves the same method.

The use of hydraulic power in energy storage has also been considered, in which the required amount of water would be stored at a high site using a small capacity pump or excess power at night followed by release of this to drive a turbine or a blower directly, thereby accelerating the air flow in a wind tunnel. This method would be very effective in a mountainous region. In concrete terms, there is the method using a hydraulic turbine and the method of direct utilization of the hydraulic pressure differential.

4.5.2 Utilization of Hydraulic Turbine

According to calculations [72], the potential energy of water stored in a spherical tank of 200 foot diameter at a height of 1,000 feet would drive a 50,000 horsepower turbine for approximately 15 minutes. It could be used as the power source for a semi-continuous wind tunnel. The output of a pump required to pump the water would constitute 7% of the turbine for driving the wind tunnel, and this would be used in continuous operation. Natual conditions would have to be used due to the great expense in construction of such a high tower and such a large tank.

For example, a water storage pond at the top of a mountain is used as the power source of the wind tunnel in the French ONERA facilities, and this method should be considered for Japan, which is rich in water.

The revolution speed of a large hydraulic turbine such as is used in a large wind tunnel is low, and it matches the requirements of the blower for a wind tunnel. Furthermore, the speed of a hydraulic turbine can be closely controlled near the designed degree, and control of the speed can be precisely implemented especially by the shock type Pelton turbine (used at ONERA) in the case of high lift, moderate output. Such properties are absent in moderate lift, high output Francis turbines, but the requirements on the turbine side can be reduced using a variable pitch blower.

4.5.3 Direct Utilization of the Hydraulic Pressure Differential

This is based on the same principle as that of a gas flow rate meter, and a conceptual figure is illustrated in figure 4.46 [16].

There is an top and bottom tank, both of which are partially filled with water. The two tanks are linked by one tube. When the valve downstream in the test section is opened, high-pressure air stored at the top of the bottom tank passes through the wind tunnel, enabling a desired flow to be achieved. The R3 tank is a tank for partial storage of the air which passed through the test section. In actual use, a piston is used to completely isolate the air and water, and a small model has been constructed in France.

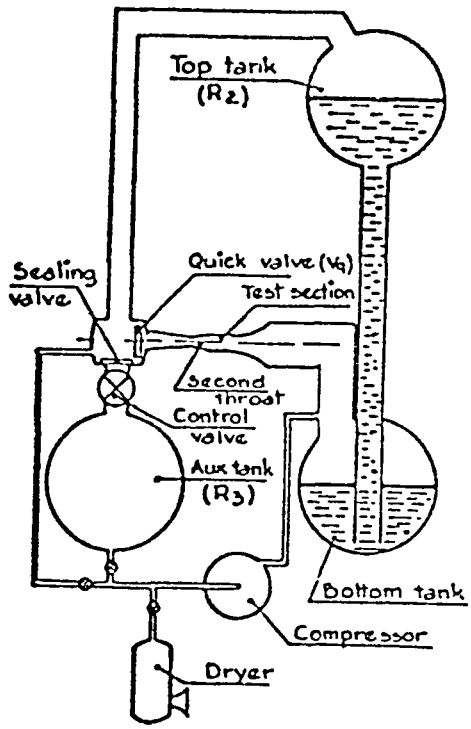

Figure 4.46 Figure of the principle in the model using the hydraulic pressure differential [16]

Figure 4.47 illustrates a vertical type large transonic wind tunnel designed in Sweden where there are site conditions favorable for this type of wind tunnel, but a horizontal wind tunnel has also been considered [73]. /31

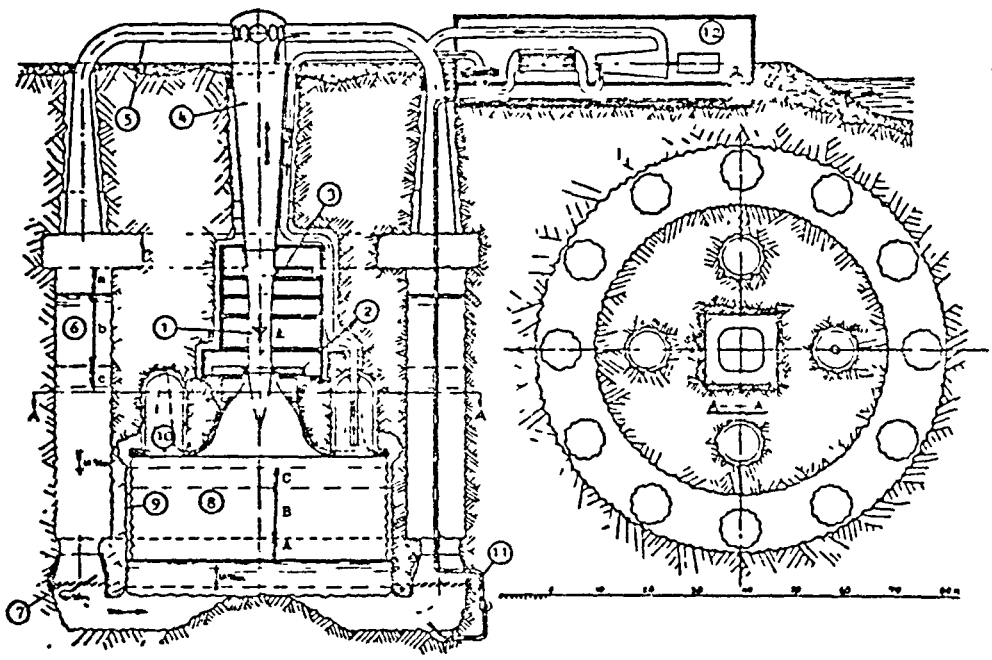

Hydraulic driven transonic tunnel meeting the LaWs specification

1. Test section 21 m²
2. Upstream shut-off valve
3. Downstream shut-off and choke valve
4. Outlet diffusor
5. Return leg (twelve in total)
6. Water storage
7. Gates for control and damping
8. Air storage
9. Bellows
10. Displacement compensation and drying bed
11. Water supply
12. Air supply

Air
- A Starting volume, initial pressure 700 kPa
- B Useful run volume, constant pressure 600 kPa
- C Stopping volume, end pressure 700 kPa

Water
- a Starting volume, initial pressure 50 kPa
- b Run period, pressure rise from 180 kPa to 400 kPa
- c Stopping volume, end pressure 410 kPa

100 kPa ≡ 1 bar

Figure 4.47 Large wind tunnel utilizing the hydraulic pressure differential [73]

The aforementioned explanations have involved various new types of wind tunnels. In addition, there is the conventional closed circuit type wind tunnel operating at normal temperature and pressure, and the intermittent blowdown type wind tunnel. Consequently, high Reynolds number transonic wind tunnels can be broadly differentiated into the following four types: (i) The normal temperature, high pressure closed circuit type (conventional type), (ii) The normal temperature, high pressure intermittent type (conventional type, induction type, Ludwieg tube, Evans Clean Tunnel), (iii) The cryogenic high pressure closed circuit type and (iv) The normal temperature, high pressure semi-continuous type (hydraulic type). There is also an example using a modified conventional intermittent blowdown type wind tunnel as a cryogenic intermittent wind tunnel [23], but this was judged to be exceptional. The types of wind tunnels suitable for Japan are examined in the next chapter.

5. The Case of Japan /32

5.1 Conditions in Various Countries and Conditions in Japan

The cryogenic high pressure circulation type wind tunnel discussed in section 4.1 is the principal type used at present. That is because this type of wind tunnel uses less energy than other types, and because the model load due to aerodynamics is low. An additional reason is that the amount of data produced is far higher than that based on the intermittent type of wind tunnel. The high Reynolds number test facilities in Europe and the United States are all of this type. In the United States, the NTF (National Transonic Facility) began operations in 1982. The decision to proceed with a cryogenic type of ETW (European Transonic Windtunnel), which is a joint project of various European countries, was made in 1977, and a 1/7 scale pilot wind tunnel (PETW) is currently under construction in Holland. The date of construction of the ETW is unclear, but construction would take four years [22]. Table 5.1 illustrates the various specifications of the NTF and ETW.

TABLE 5.1 NTF AND ETW

	NTF (U.S.)	ETW (Europe)
test section (m)	2.5 x 2.5	1.95 x 1.65
Mach number	0.2 to 1.2	0.15 to 1.35
Peak Reynolds number	120×10^6	40×10^6
Designed Reynolds number	(120×10^6)	25×10^6
Wind tunnel internal pressure	1 to 9	1 to 4.5
output of motor for blower (MW)	97	37
LN_2 tank	$1,136.5m^3$	1,200 tons
LN_2 production plant	unknown	120 tons/day
data production	8,000 polar curves/year	5,000 polar curves/year
operational date	1983	unknown

The wind tunnel construction projects in socialist countries are unknown.

In Japan, joint construction with other countries is nearly impossible because of circumstances including the site of construction and means of communications since there are no advanced countries nearby, in contrast with Europe. Conversely, there are signs of the development of an aircraft industry, and it will be an industry of future emphasis in Japan. Since wind tunnels constitute an indispensable facility for the development of aircraft, wind tunnels of the same level of performance as those in Europe and the United States are essential [74,75].

A two-dimensional wind tunnel operating since 1979 by the National Aerospace Laboratory has served as the high Reynolds number test facility in Japan [76,77]. This is a transonic wind tunnel for testing only the wing section, which is one element of an actual aircraft, at high Reynolds number (peak of 40×10^6), but it is incapable of testing full-scale configurations at high Reynolds numbers.

Thus, construction of a three-dimensional wind tunnel independently by Japan is necessary, considering the aforementioned circumstances. An example of the construction period would be 1986-89 in literature [75], but preparatory

experiments must be conducted early, considering the preliminary stage.

First, a determination of the basic specifications, including the peak Reynolds number, must be made, leaving aside the structure, in construction of such a large wind tunnel. A pilot wind tunnel of the determined type would be constructed after evaluation of the principal specifications and type of wind tunnel in accordance with that, and the design data, including performance, etc., would be determined using this, followed by construction of the full-scale wind tunnel. The duration of this sequence could be shortened by using the data from various advanced countries in this procedure, but the preliminary period in Japan would have to be four to five years, and three to four years would be necessary for wind tunnel construction, considering that research and development into cryogenic wind tunnels using liquid nitrogen began in the United States in 1971, and considering the research [78] which has been conducted from various aspects. The technical disparity involving aircraft between Japan and Europe-America would become even wider if work is not commenced soon.

5.2 Basic Specifications of High Reynolds Number Wind Tunnel

There are two factors which have a great influence on the scale and type of wind tunnel, leaving aside cost. One is the /33
maximum Reynolds number and the other is the productivity of data. Even if the Mach number range were to vary somewhat, there would not be a major effect so long as the tests are in the transonic region.

First, we will consider the maximum Reynolds number. At least, testing at a Reynolds number of 40×10^6 is essential considering the explanation in chapter 2 and the performance of NTF and of ETW (table 5.1). This number is the peak Reynolds

number of NAL two-dimensional wind tunnel for testing wings which is currently in operation, and this Reynolds number is needed to make relation with various other data. In addition, the acquisition of the same level of performance as that of wind tunnels in Europe and the United States would be very useful when carrying out joint international development of aircraft. Furthermore, acquisition of the same level of performance would enable to compare test results with other test results obtained in foreign wind tunnels, and would be useful is raising the technology of wind tunnel experiments.

Achievement of a maximum Reynolds number would be achieved through enlargement of wind tunnels, raising the pressure, lowering the temperature or through combinations of these. It is one important point in the selection of the type of wind tunnel, and it is evaluated in section 5.3.

We will next consider data productivity. Since aerodynamic data on actual configurations are usually expressed by polar curves, the amount of data produced can be determined by the number of polar curves. Data productivity is emphasized in the NTF and ETW projects, and the number of polar curves acquired annually as well as the operating expense per polar curve have been evaluated [16].

The most modern type of high speed instrumentation system is used, of course, to raise the data production. Usually, 15 seconds of running time are required if one polar curve is composed of data with 20 points of angles of attack in a six component force test and if a high speed instrumentation system is used. One polar curve constitutes data based on 10 points of angles of attack in the case of pressure distribution test, and 60 seconds of running time are required. The time required for setting and adjustment of the flow during each instrumentation period is also needed, and in the ETW project, for example, 30

polar curves are produced daily in running time of 30 minutes daily. The continuous type 2 m x 2 m transonic wind tunnel of the National Aerospace Laboratory produces 10 to 15 polar curves (half as many in pressure tests) through running time of four hours daily, and while for the pressure test data which are produced in the intermittent two-dimensional wind tunnel for high Reynolds number tests, one polar curve would be produced at the maximum Reynolds number test state.

In general, there are cases in which testing involving 10 seconds of running time using the intermittent type wind tunnel would be impermissible considering the extent of data productivity since the data productivity the intermittent type wind tunnel is 1/2 to 1/6 that of the continuous type wind tunnel [7].

However, daily production of 20 polar curves (pressure tests) would be possible even with the intermittent type wind tunnel if the high speed instrumentation system is used, or if high-speed setting and adjustment of the flow is implemented [16].

5.3 Selection of the Type of Wind Tunnel

Although the most suitable type of wind tunnel from among the various types discussed in chapter four would depend on the objectives of use of the wind tunnel and with the site conditions, etc. when considering three-dimensional high Reynolds number wind tunnels, the principal items which should be evaluated are as cited below.

(a) performance at designed test conditions (including flow quality)
(b) possible testing range
(c) performance at test conditions outside of the designed test conditions
(d) convenience and safety of use
(e) construction costs
(f) operating and maintenance costs

(operating energy costs, maintenance costs, production costs of test models etc.)

The meaning of (c) is, for example, the case of low Reynolds number operation of high Reynolds number wind tunnel then, testing becomes generally very simple (normal temperature operation of cryogenic wind tunnels) or the running time becomes very long (conventional intermittent wind tunnels), but some wind tunnels, such as the Ludwieg tube, do not vary greatly their performance. Item (d) is convenience and safety during wind tunnel experiments, and this includes ease of model replacement, use of conventional instrumentation as well as ease and safety of starting or terminating of blow (29).

Table 5.2 illustrates the aforementioned properties in the various types of wind tunnels. Figure 5.1 (a) (b) (18), which used the construction costs and operating energy costs during planning of the ETW project, was also consulted.

As table 5.2 indicates, the advantages and disadvantages involving maximum Reynolds number achieved, ease of use, safety in use and model production costs etc. are determined by utilizing either the cryogenic type or normal temperature type. Furthermore, it can be considered that table 5.2 shows the classifications based on differences in the mode of driving the gas, excluding type 1, and the drive methods in types 2 through 8 using cryogenic gas have also been considered (type 1 is a cryogenic gas using the drive method of type 2). An example would be the intermittent blowdown type cryogenic wind tunnel (8,23) discussed in chapter 4. "Proliferation of uncertain items" in table 5.2 is the tunnel with few experimental results in contrast to the complexity of the facilities, and it /34 signifies a long preliminary period involving tests based on pilot wind tunnels etc.

TABLE 5.2 COMPARISON OF VARIOUS TYPES OF WIND TUNNELS

1 番号	1	2	3	4	5	6	7	8
2 型式	3 常温連続回流	4 従来型連続回流	5 従来型間欠吹出	6 誘導 IDT	ルートビーク管 7 LT	エバンス風洞 8 ECT	9 水力タービン半連続回流	10 水圧利用
11 使用気体	12 低温窒素	13 常温空気	14 同左	同左	同左	同左	同左	同左
15 到達最高レイノルズ数	○	△	△	△	△	△	△	△
16 風洞規模	○	×	△	△	×	△	×	×
17 データ生産性（通風時間）	○	○	×	×	×	×	○	△
18 オフデザイン性能	○	○	○	○	×	○	○	○
19 使用上，便利さ	×	○	○	○	○	○	○	○
20 安全性	×	○	○	○	○	○	○	○
21 建設費	○	×	△	△	△	△	×	×
22 運転エネルギ	△	×	△	×	△	○	×	×
23 保守・維持	×	△	△	○	○	△	△	△
24 模型製作	○	△	△	△	△	△	△	△
25 不確定項目の多さ	×	○	○	△	△	△	○	△

26 注1 ○ 良，△ 許容，× 悪い
27 注2 flow quality は明確な結論がないので省略

1 number
2 model type
3 cryogenic continuous closed-circuit
4 conventional type continuous closed-circuit
5 conventional type intermittent closed-circuit
6 induction driven tunnel, IDT
7 Ludwieg tube LT
8 Evans Clean Tunnel ECT
9 hydraulic turbine semi-continuous closed-circuit
10 utilization of hydraulic pressure
11 gas used
12 cryogenic nitrogen
13 normal temperature air
14 same as at left
15 peak Reynolds number attained
16 scale of wind tunnel
17 data production (running time)
18 off design performance
19 convenience in use
20 safety
21 construction costs
22 operating energy
23 repairs, maintenance
24 model production
25 proliferation of uncertain items
26 Note 1. O good, Δ permissible, × poor
27 Note 2. Flow quality was omitted since there is no definite conclusion.

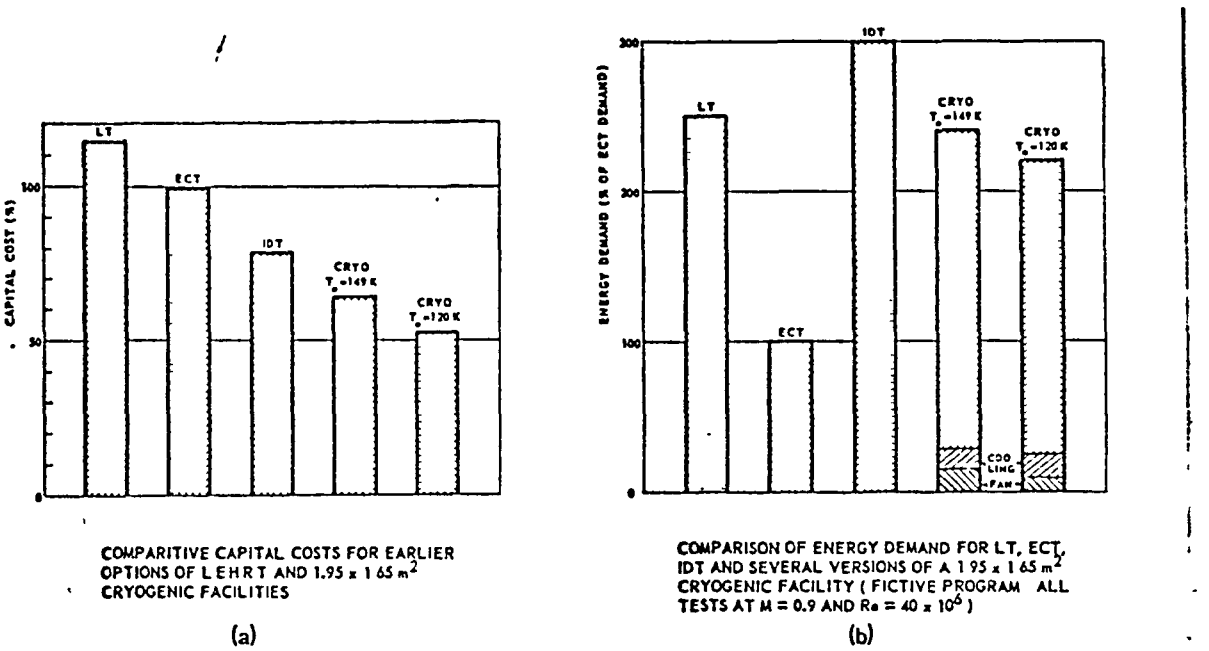

COMPARITIVE CAPITAL COSTS FOR EARLIER OPTIONS OF LEHRT AND 1.95 x 1.65 m^2 CRYOGENIC FACILITIES

(a)

COMPARISON OF ENERGY DEMAND FOR LT, ECT, IDT AND SEVERAL VERSIONS OF A 1.95 x 1.65 m^2 CRYOGENIC FACILITY (FICTIVE PROGRAM ALL TESTS AT M = 0.9 AND Re = 40 x 10^6)

(b)

Figure 5.1 Construction costs (a) and energy demand (b) (18)

The most suitable wind tunnel types for given conditions could be selected using table 5.2. Actually, trade-offs must be made using more precise figures, but in the case of Japan, when considering a three-dimensional high Reynolds number transonic wind tunnel with maximum Reynolds number of 40 x 10^6 and Mach numbers of 0.2 to 1.2, the author believes that the tunnel candidate which is used to development of aircraft would be the following three types.

(1) cryogenic, continuous closed circuit type

(2) hydraulic turbine continuous closed circuit type

(3) conventional continuous closed circuit type.

/35

In order to minimize the operating energy, the pressure loss of the flow passages must be reduced as much as possible in candidates (2) and (3).

6. Conclusions

The features of various types of wind tunnels have been described, reconfirming the necessity of transonic, high Reynolds number tests. In addition, the items requiring verification have been illustrated in the case of the high Reynolds number wind tunnel construction in Japan. An evaluation organization must be drawn up as soon as possible because of the prolonged preliminary period.

REFERENCES

1) Pope, A. M. S.: Wind Tunnel Testing, John Wiley & Sons, Inc., New York (1961/10).
2) Pankhurst, R. C. and Holder, D. W.: Wind Tunnel Technique, Sir Isaac Pitmann & Sons Ltd., London, (1952).
3) Dayman, B. Jr. and Fiore, A. W.: Aerodynamic Testing and Simulation: Saving Lives, Time, and Money, Astro. & Aero., Vol. 12, No. 6 (1974/6).

4. N. Hirose: Prospects of Calculated Aerodynamics, Journal of the Japan Society for Aeronautical and Space Sciences, Vol. 28, No. 318 (July, 1980)

5) Heppe, R. R. et al.: New Aeronautical Facilities We Need Them Now, Astro. and Aero., Vol. 6, No. 3 (1968/3).
6) Lukasiewicz, J.: The Need for Developing a High Reynolds Number Transonic Wind Tunnel in the U.S., Astro. and Aero., Vol. 9, No. 4 (1971/4).
7) Whitfield, J. D. et al.: High Reynolds Number Transonic Wind Tunnels Blowdown or Ludwieg Tube?, AGARD CP-83-71, Paper No. 29 (1971/8).
8) Kilgore, R. H. et al.: The Cryogenic Wind Tunnel Concept for High Reynolds Number Testing, NASA TN D-7762 (1976).
9) Jones, J. L.: The Transonic Reynolds Number Problem, NASA CP-2009, pp. 1 ~ 18 (1977).
10) Lukasiewicz, J. (ed): Aerodynamic Test Simulation: Lessons from the Past and Future Prospects, AGARD R603 (1972/12).
11) Loving, D. L.: Wind Tunnel-Flight Correlation of Shock Induced Separated Flow, NASA TN D-3580 (1966).
12) Jones, J. L.: Problems of Flow Simulation in Wind Tunnels, AIAA Paper No. 69-660 (1969/6).
13) Igoe, W. B. and Baals, D. D.: Reynolds Number Requirements for Valid Testing at Transonic Speeds, AGARD CP-83-71, Paper No. 5 (1971/8).

14) Roepke, R. G.: The High Reynolds Number Transonic Wind Tunnel HIRT Proposed as Part of the National Aeronautical Facilities Program, AIAA Paper No. 72-1035 (1972/9).

15) Küchemann, D. (ed): Problems of Wind Tunnel Design and Testing, AGARD R-600 (1973/12).

16) Hills, R.: The Need for a Large Transonic Wind Tunnel in Europe: A Summary of the Report of an AGARD Working Group (La Ws), AIAA Paper No. 74-630 (1974).

17) Kilgore, R. A.: Development of the Cryogenic Tunnel Concept and Application to the U.S. National Transonic Facility, AGARD-AG-240, Paper No. 2 (1980).

18) Hartzuiker, J. P.: Towards New Transonic Wind Tunnels, AGARD-AG-240, Paper No. 3 (1980).

19) Treon S. L. and Hofstetter, W. R.: On the Use of Freon-12 for Increasing Reynolds Number in Wind Tunnel Testing of Three-Dimensional Aircraft Models at Subcritical and Supercritical Mach Numbers, AGARD CP-83, Paper No. 27 (1971).

20) Igoe, W. B.: Characteristics and Status of the U.S. National Transonic Facility, AGARD-LS-111, Paper No. 17 (1980).

21) Luneau, J., Rochas, N. and Kirrmann, C.: Preliminary Study of the Injection Process of LN_2 in a Cryogenic Wind Tunnel, 1st Int. Symp. on Cryogenic Wind Tunnels, Paper No. 14 (1979).

22) Hartzuiker, J. P. and North, R. J.: The European Transonic Wind Tunnel ETW, AGARD-LS-111, Paper No. 16, (1980).

23) Cadwell, J. D.: Progress Report on the Douglas Aircraft Company Four-Foot Cryogenic Wind Tunnel, AGARD-LS-111, Paper No. 18 (1980).

24) Goodyer, M. J. and Kilgore, R. A.: The High Reynolds Number Cryogenic Wind Tunnel, AIAA Paper No. 72-995 (1972).

25) Kilgore, R. A.: Design Features and Operational Characteristics of the Langley Pilot Transonic Cryogenic Tunnel, NASA TM X-72012 (1974).

26. N. Yoshisawa: Private communication.
27. I. Kawashima, M. Tani, N. Yoshisawa: On Cryogenic Wind Tunnel Operations, Shock Engineering Symposium, pp. 196-202 (1980)

28) DFVLR-Nachrichten, Heft 31 (November 1980), pp. 9 ~ 10.
29) Voth, R. O. and Strobridge, T. R.: Cryogenic Design and Safety Review NASA-Langley Research Center 0.3 Meter Transonic Cryogenic Tunnel, NBSIR 77-857 (1977).
30) Knowler, A. E. and Holder, D. W.: Efficiency of High-Speed Wind Tunnels of the Induction Type, ARC R. & M. No. 2448 (1954).
31) Muhlstein, L., Petroff, D. N. and Jillie, D.: Experimental Evaluation of an Injector System for Powering a High Reynolds Number Transonic Wind Tunnel, AIAA Paper No. 74-632 (1974).
32) Michel, R., Mignosi, A. and Quémard, C.: The Induction Driven Tunnel T2 at ONERA-CERT: Flow Qualities, Testing Techniques and Examples of Results, AIAA Paper No. 78-767 (1978).
33) Michel, R.: The Development of a Cryogenic Wind Tunnel Driven by Induction: Flow Control and Instrumentation Studies in a Pilot Facility at ONERA/CERT, AGARD-LS-111 Paper No. 13 (1980).
34) Kilgore, R. A., Adcok, J. B. and Rey, E. J.: Simulation of Flight Test Conditions in the Langley Pilot Transonic Cryogenic Tunnel, NASA TN D-7811 (1974).
35) Howell, R. R. and Mckinney, L. W.: The U.S. 2.5-Meter Cryogenic High Reynolds Number Tunnel, NASA CP-2009, pp. 27 ~ 51 (1976).
36) Kilgore, R. A.: Cryogenic Wind Tunnel Technology, NASA CP-2009, pp. 53 ~ 63 (1976).
37) Ludwieg, H.: Tube Wind Tunnel a Special Type of Blowdown Wind Tunnel, AGARD Rep. 143 (1957).
38) Davis, J. W.: A Shock Tube Technique for Producing Subsonic, Transonic, and Supersonic Flows with Extremely High Reynolds Numbers, AIAA Paper No. 68-18 (1968/1).
39) Felix, A. R.. MSFC High Reynolds Number Tube Tunnel, AGARD CP-83-71 Paper No. 30.
40) Lorentz-Meyer, W.: Parametric Investigation of the Large Transonic Ludwieg Tube Wind Tunnel, DFVLR 251 74A22 (1974/4).

41. K. Takashima, K, Hakii , T. Aoki: Properties of Transonic Ludwieg Tube, National Aerospace Laboratory Technical Report TR-441, (January, 1976)

42. K. Takashima et al.: On the Properties of the 120 mmx 360 mm Ludwieg Tube of the National Aerospace Laboratory and Transonic Two-Dimensional Wing Tests, National Aerospace Laboratory Technical Memorandum TM-383, (June, 1979)

43) Takashima, K.: On the Starting Process of a Transonic Ludwieg Tube Wind Tunnel, Trans. Japan Soc. Aero. Space Sci., Vol. 22, No. 58 (1980).

44. K. Takashima, N. Hara , T. Aoki: Visualization of Air Flow in Ludwieg Tube by Laser Holographic Interferometer, National Aerospace Laboratory Technical Report TR-609, (May, 1980).

45) Cable, A. J., Cox, R. N.: The Ludwieg Pressure-tube Supersonic Wind Tunnel, The Aero. Quart. Vol. 14, Part 2 (1963/5).

46) Grauer-Carstensen, H. et al.: Some Aspects Important to the Design and Performance of a Large Transonic Ludwieg Tube Wind Tunnel, DFVLR 251 73A09 (1973/3).

47) Davis, J. W., Gwin, H. S.: Feasibility Studies of a Short Duration High Reynolds Number Tube Wind Tunnel, NASA TM X-53571 (1968).

48) Starr, R. F. and Schueler, C. J.: Experimental Studies of a Ludwieg Tube High Reynolds Number Transonic Tunnel, AIAA Paper No. 73-212, (1973).

49) Shope, F. L.: Mathematical Model for the Starting Process of a Transonic Ludwieg Tube Wind Tunnel, J. Aircraft, Vol. 14, No. 6 (1977).

50) Warmbrod, J. D.: A Theoretical and Experimental Study of Unsteady Flow Process in a Ludwieg Tube Wind Tunnel, NASA TN D-5469 (1969).

51) Becker, E.: Das Anwachsen der Grenzschicht in und Hinter Einer Expansionswelle, Ing-Arch., Part XXV, Heft 3 (1957).

52) Mirels, H.: Boundary Layer Behind Shock or Thin Expansion Wave Moving into Stationary Fluid, NACA TN 3712 (1956).

53) Piltz, E.: Boundary Layer Effects on Pressure Variations in Ludwieg Tubes, AIAA J. Vol. 10, No. 8 (1972).

54) Pugh, P. G., Grauer-Carstensen, H., Quemard, C.: An Investigation of the Quality of the Flow Generated by Three Types of Wind Tunnel (Ludwieg Tube, Evans Clean Tunnel and Injector Driven Tunnel) AGARD AG 240, pp. 1-1 ~ 1-23 (1979/11).

55) Davis, J. W. and Graham, R. F.: High Reynolds Number Experimental Data for Forebody Axial Force, AIAA J., Vol. 11, No. 3 (1973).

56) Dumitrescu, L. Z.: A Large-Scale Aerodynamic Test Facility Combining the Shock and Ludwieg Tube Concepts, Shock Tubes and Waves, Magnes Press, Hebrew Univ., Jerusalem (1980).

57. Fu-Hsing Tsien: Private Communication

58) Srinivas, K.: Private Communication.

59) Pankhurst, R. C. (ed): Large Wind Tunnels: Required Characteristics and the Performance of Various Types of Transonic Facility, AGARD R-615 (1974).

60) Hendershot, K. C. and Drzewiecki, R. F.: Techniques Used for the Investigation of Aerodynamic Loads Induced on a Rocket-Powered Vehicle during Deployment of an Extendible Nozzle, Proc. AIAA 9th Aero Testing Conf., Arlington (1976).

61. K. Takashima: On Experiments using Ludwieg Tube, Journal of the Japan Society for Aeronautical and Space Sciences, Vol. 25, No. 286, (November, 1977).

62) Evans, J. Y. G.: A Scheme for a Quiet Transonic Flow Suitable for Model Testing at High Reynolds Number, RAE TR 71112 (1971/5).

63. T. Aoki, K. Takashima: Prolongation of Duration of Ludwieg Tube by Reservoir-Orifice Method, National Aerospace Laboratory Technical Report TR-612, (May, 1980)

64) Pugh, P. G.: Experimental Trials of a Novel (ECT) Drive System for a Transonic Wind Tunnel, RAE TR 71208 (1971/10).

65) Pugh, P. G.: The Development of an Efficient and Economical System for the Generation of Quiet Transonic Flows Suitable for Model Testing at High Reynolds Number, AGARD-R-600 (1973/12).

66) Pugh, P. G., Beckett, W. A. and Gell, T. G.: The ECT Drive System: A Demonstration of its Practicability and Utility, AGARD-CP-174 (1976/3).

67) Lukasiewicz, J.: A Critical Review of Development of Experimental Methods in High-Speed Aerodynamics, Prog. Aero. Sci., Vol. 14 (1973), pp. 1 ~ 26.

68. G. Kamimoto: Instrumentation in Shock Tube, Journal of the Japan Society for Aeronautical and Space Sciences, Vol. 11, No. 117, pp. 18-25 (October, 1963).

69) Barbour, N. M. and Imrie, B. W.: A Reservoir/Orifice Technique for Extending the Useful Running Time of a Ludwieg Tube, Modern Developments in Shock Tube Research, Proc. 10th Int. Shock Tube Symp. (1975), pp. 252 ~ 259.

70. H. Matsuo, S. Kawagoe, K. Nishizaki, N. Kondo: Prolongation of the Duration of Uniform Flow in a Ludwieg Tube by the Reservoir-Orifice Method (First Report, In the case of Uniform Orifice of Aperture Area), Transaction of the Japan Society of Mechanical Engineers, Vol. 44, No. 381, pp. 1581-1587, (May, 1978)

71. H. Matsuo, S. Kawagoe, K. Nishizaki, N. Kondo: Prolongation of the Duration of Uniform Flow in a Ludwieg Tube by the Reservoir-Orifice Method (Second Report, In the case of Variable Orifice of Aperture Area), Transaction of the Japan Society of Mechanical Engineers, Vol. 45, No. 391, pp. 323-330, (March, 1979)

72) Baals, D. D. and Stokes, G. M.: A Facility Concept for High Reynolds Number Testing at Transonic Speeds, AGARD CP-83-71 Paper No. 28 (1971/8).

73) Nelander, C. and Önerby, B: Application of the Gasometer Storage Concept to a Transonic Wind Tunnel Meeting the LAWs Specification, AGARD R-615, Paper No. 3 (1974/6).

4. Choki Koso Bunkakai: Survey Data Collection concerning Current Circumstances and Prospects for Aerospace Technology, Aircraft-Electronic Technical Examination Committee, National Aerospace Technical Committee, (November, 1980)

75. Choki Koso Iinkai: 1979 Survey Report on Long-Term Plans (Abstract), Japan Aerospace Industrial Committee, (March, 1980)

76. H. Endo: On Two-Dimensional Wind tunnels, Journal of the Japan Society for Aeronautical and Space Sciences Vol. 26, No. 299, (December, 1978).

77. Kuki Rikigaku Dainibu, The Second Aerodynamics Division: Structure and Properties of the Two-Dimensional Transonic Wind Tunnel of the National Aerospace Laboratory, National Aerospace Laboratory Technical Memorandum TR-647, (March, 1981)

78) Tuttle, M. H. and Kilgore, R. A.: Cryogenic Wind Tunnels – A Selected, Annotated Bibliography, NASA TM 80168 (1979/10).

End of Document